Calcification, Ossifications, Matrices, Radiodense Foreign Bodies and Their Mimics

CALCIFICATION, OSSIFICATIONS, MATRICES, RADIODENSE FOREIGN BODIES, AND THEIR MIMICS

ANTHONY A. MANCUSO

KEY POINTS

- Calcification, ossification, and the presence of a matrix are frequently crucial to the diagnostic process.
- Calcification, ossification, and matrices are more easily and accurately appreciated on computed tomography.
- Radiodense foreign bodies, blood, impacted secretions, and reactive changes may mimic calcification and ossification. This may impede or enlighten the diagnostic process.
- Protocols for imaging approaches to clinical problem solving must take into account the relative strength of computed tomography over magnetic resonance imaging for identifying calcification, ossification, matrices, and foreign bodies that are radiodense on computed tomography.

The presence of calcification, ossification, or their mimics is often not important if such findings are physiologic or just part of the natural aging process (Fig. 12.1). Sometimes, calcification, when present, is not a critical factor in evaluating a related disease process (Fig. 12.2). However, sometimes calcification can prove crucial for differential diagnosis and medical decision making (Fig. 12.3). The cause of some calcifications often remains unknown. In all cases, calcifications and all calcified matrices are better seen and appreciated for what they are on computed tomography (CT) and plain films than magnetic resonance (MR), and this becomes a critical issue for planning the proper imaging approach to clinical problems. The latter point is the main issue of interest in this introductory material. Calcifications are marginally appreciable on ultrasound.

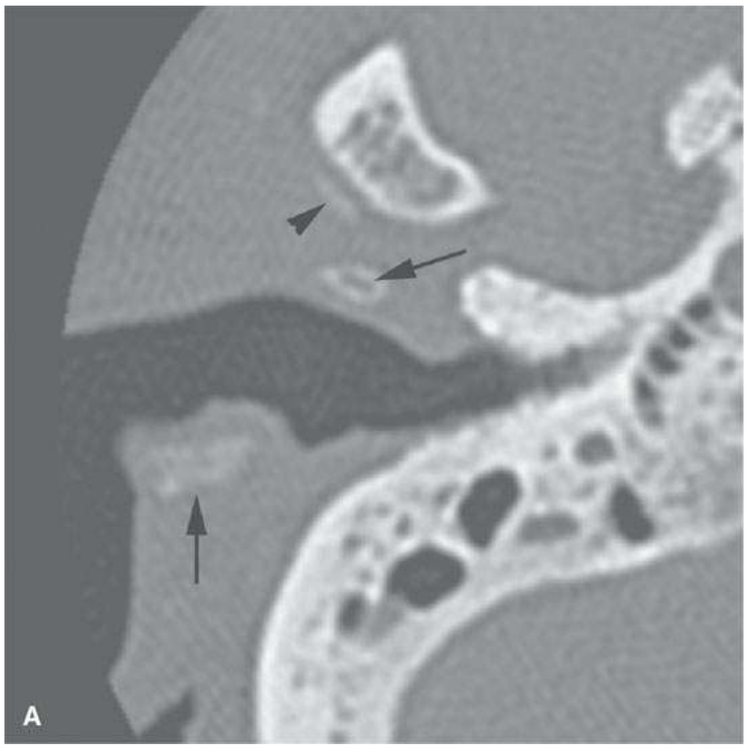

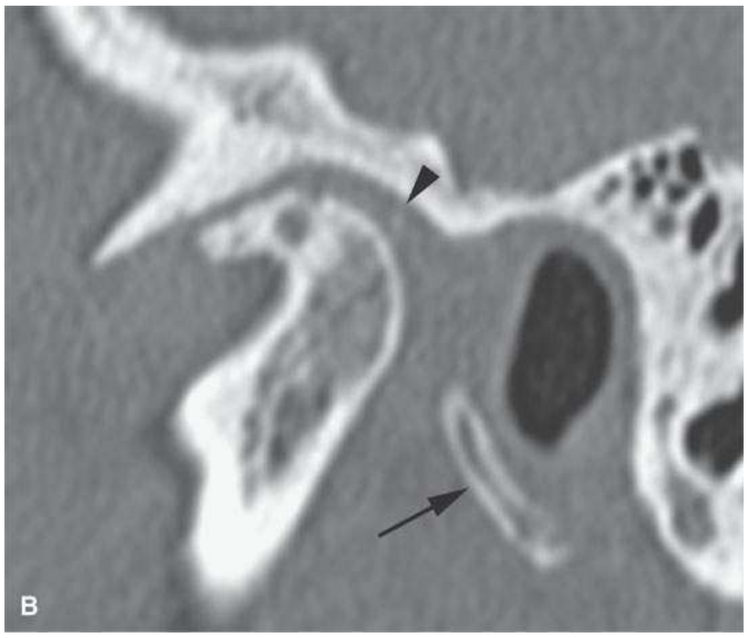

FIGURE 12.1. Computed tomography at bone windows showing calcification of the ear cartilage, a normal variant *(arrows)*, and dystrophic temporomandibular joint disc and capsule calcification *(arrowheads)*.

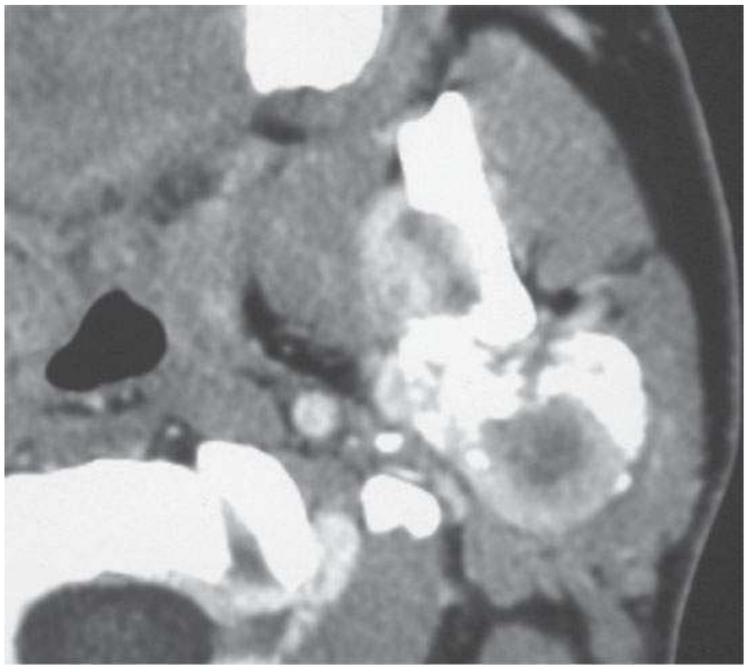

FIGURE 12.2. Contrast-enhanced computed tomography of a partially calcified synovial cell sarcoma where the likely dystrophic tumoral calcification is not helpful in differential diagnosis.

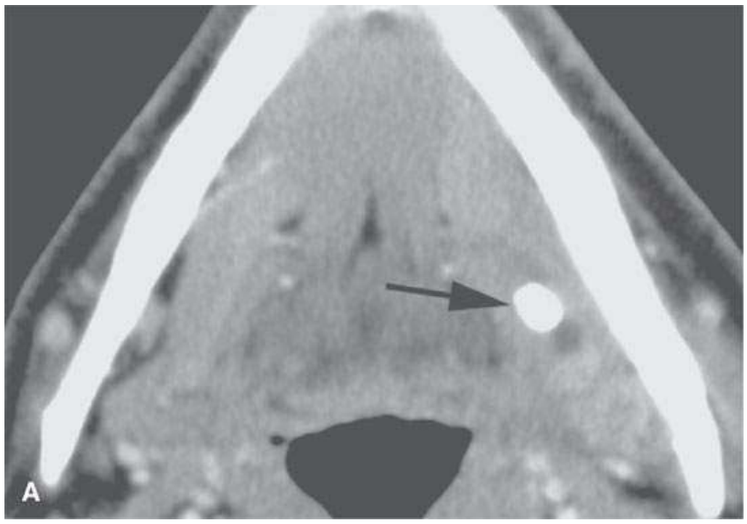

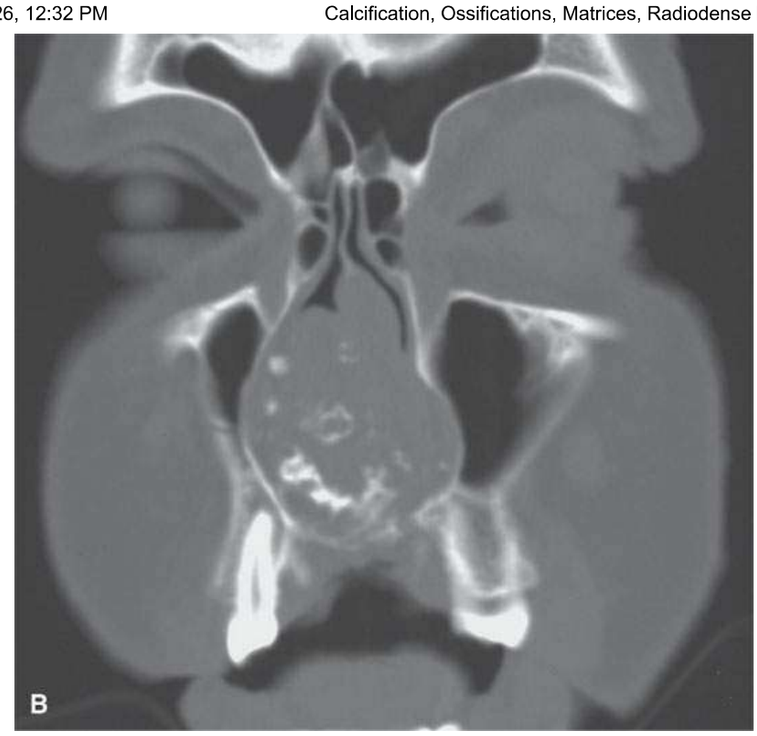

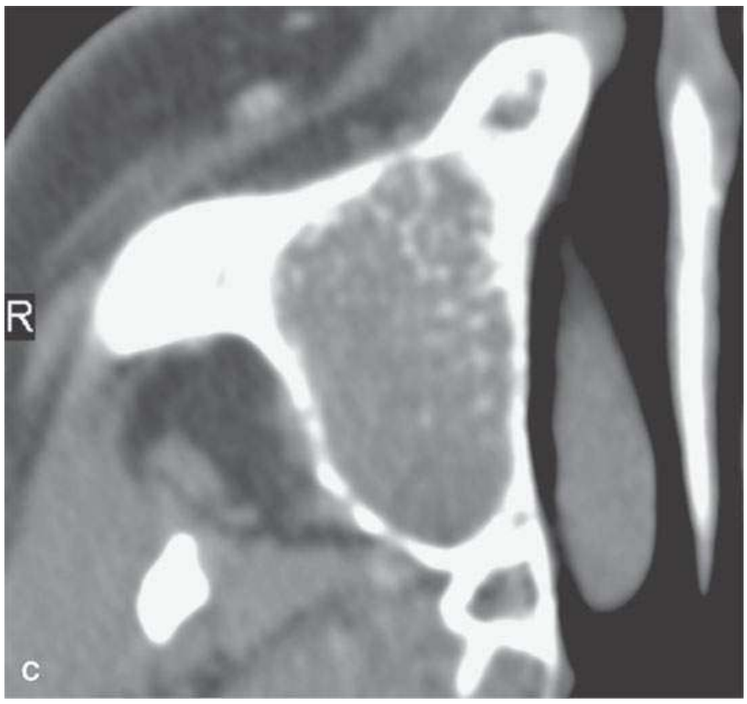

FIGURE 12.3. Examples where magnetic resonance would likely not make as good a diagnosis based on recognizing calcification and mineralization as computed tomography (CT) and where this information is critical to proper diagnosis. **A**: Contrast-enhanced CT of low-grade sialoadenitis presenting as a submandibular mass—the stone *(arrow)* and ductal dilatation is obvious on CT and might be more difficult to detect with magnetic resonance imaging (MRI) or ultrasound. **B**, **C**: CT makes the specific diagnosis of chondrosarcoma of the nasal septum **(B)** and chondroblastoma or at least a chondroid matrix lesion **(C)** that is unlikely to have been as apparent a diagnosis on MRI.

THINGS THAT MAY LOOK CALCIFIC BUT ARE NOT

The range of CT density that might appear on images as calcific is wide. Sometimes, dense keratin debris in lymph nodes, densely desiccated secretions, or metals other than calcium manifest a similar density, signal intensity, or pattern of echogenicity— things that may look like calcifications but are not that at all (Figs. 12.4A,B). Small metallic foreign bodies and even wood can mimic calcific density (Fig. 12.5) on CT.1 Focal areas of contrast enhancement and even normal vessels may mimic or mask calcification from accurate observation. Acute or subacute blood products can be mistaken for calcification (Fig. 12.5B). Sometimes, the foreign bodies are actually calcified even though they originate extrinsically; this appearance may evolve over time (Fig. 12.6). It is particularly difficult to recognize foreign bodies on magnetic resonance imaging (MRI) compared to CT; however, MRI may provide clues to their nature. The variations that such findings can create on MRI can be even more confusing (Fig. 12.7).

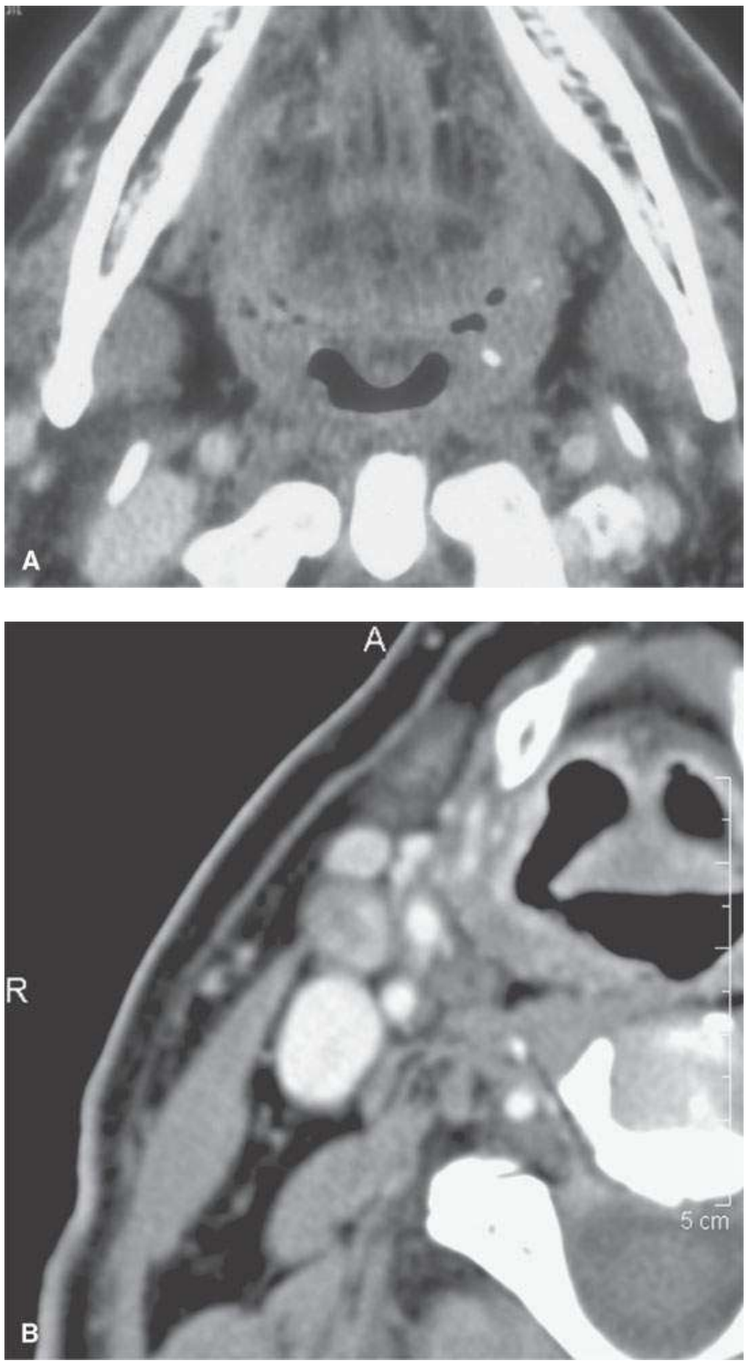

FIGURE 12.4. Examples of keratin and other "debris" mimicking calcification. **A:** Contrast-enhanced computed tomography (CECT) of normal variant of impacted high-density foci of material in tonsillar crypts. **B:** CECT of nodes surgically proven to contain high-density keratin debris and no calcification following radiotherapy.

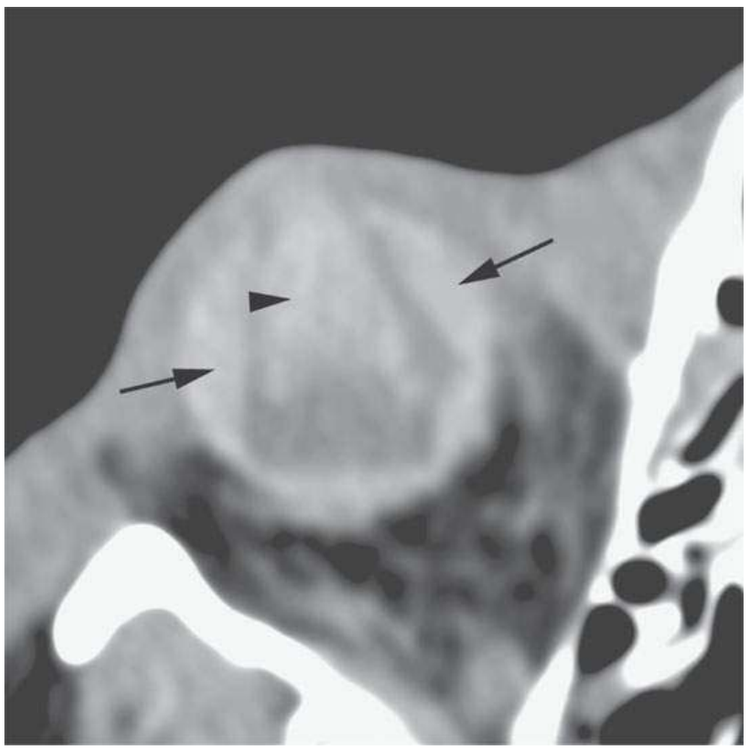

FIGURE 12.5. Computed tomography of choroidal hemorrhage *(arrows)* as well as anterior and posterior chamber and vitreous hemorrhage that could be a

calcification or otherwise mineralized foreign body *(arrowhead)*. Compare this figure with Figure 12.16.

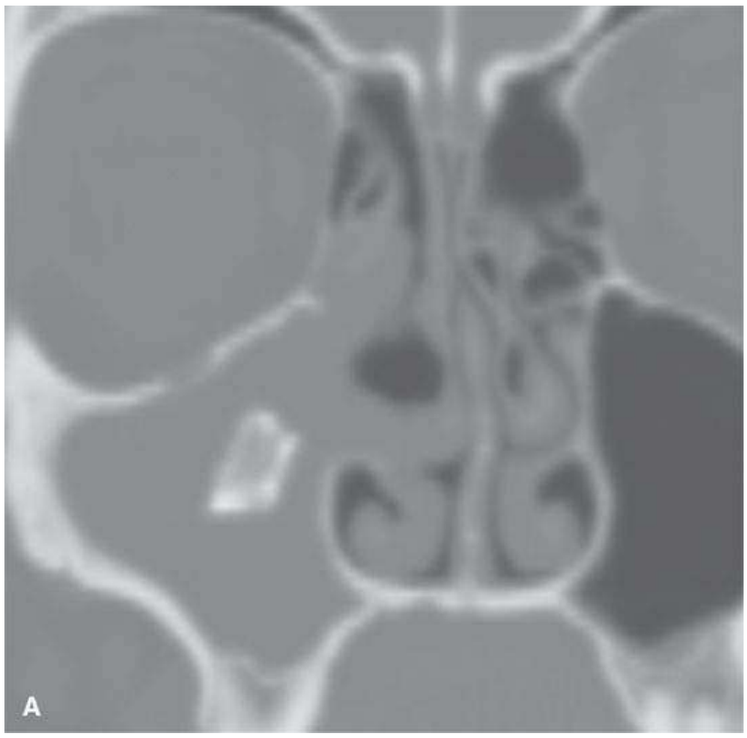

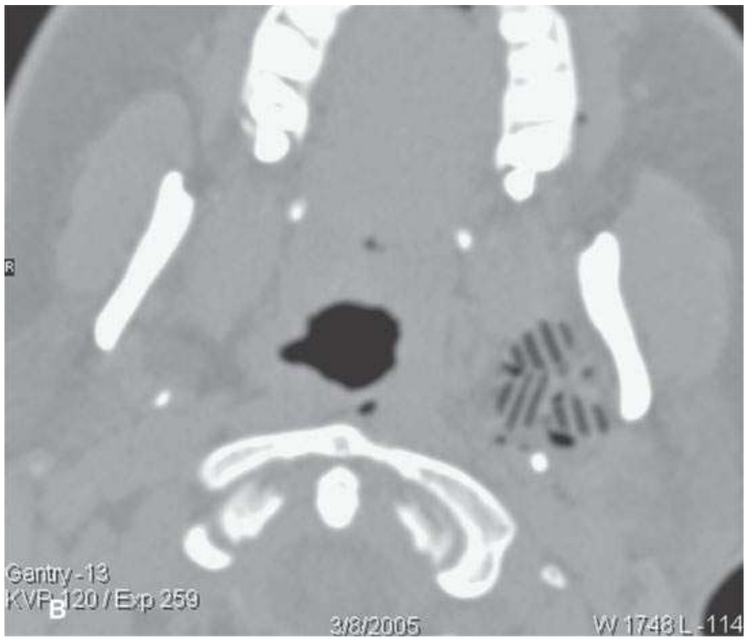

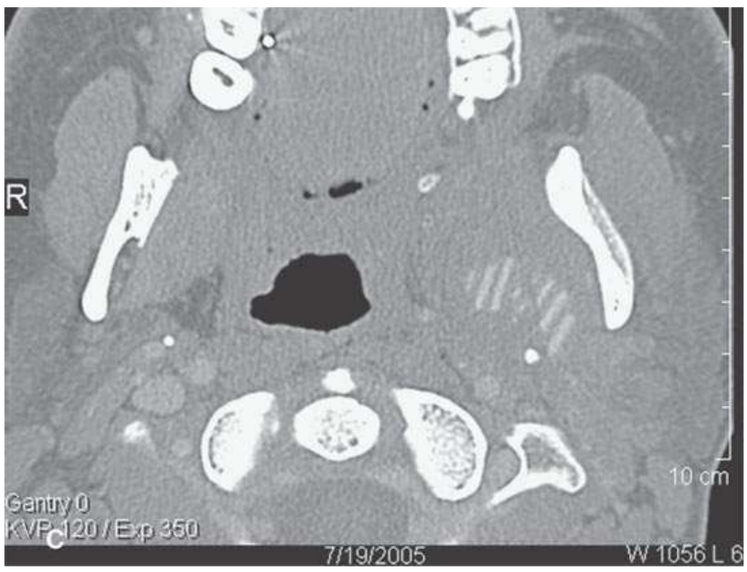

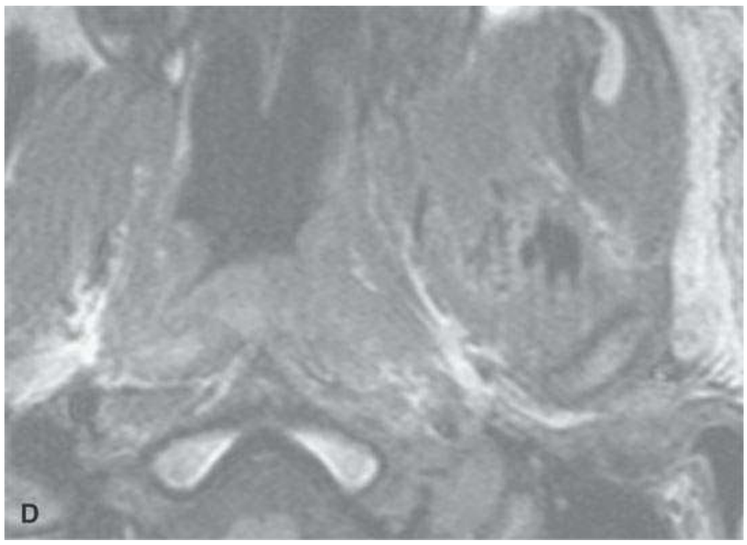

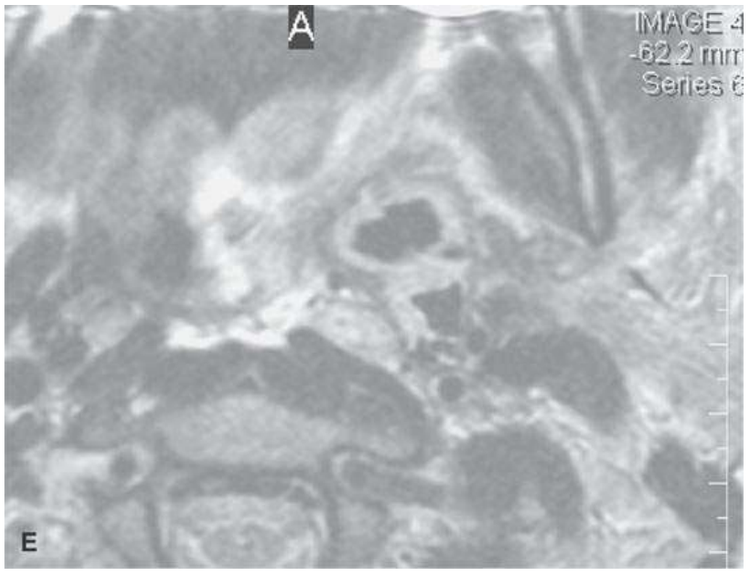

FIGURE 12.6. Calcified foreign bodies. **A:** Computed tomography (CT) of calcified surgical material that incited this chronic sinusitis left after an endoscopic sinus surgery procedure. **B–E:** Non–contrast-enhanced CT and magnetic resonance imaging (MRI) of a patient who had a piece of a fence post penetrate from the orbit to the deep facial soft tissues. In **(B)**, the air pattern shows the wood. Weeks later in **(C)**, the foreign body has mineralized. In **(D)** and **(E)**, the MRI does not really provide as definitive overall evaluation of the situation, but is does nicely demonstrate the surrounding soft tissue response.

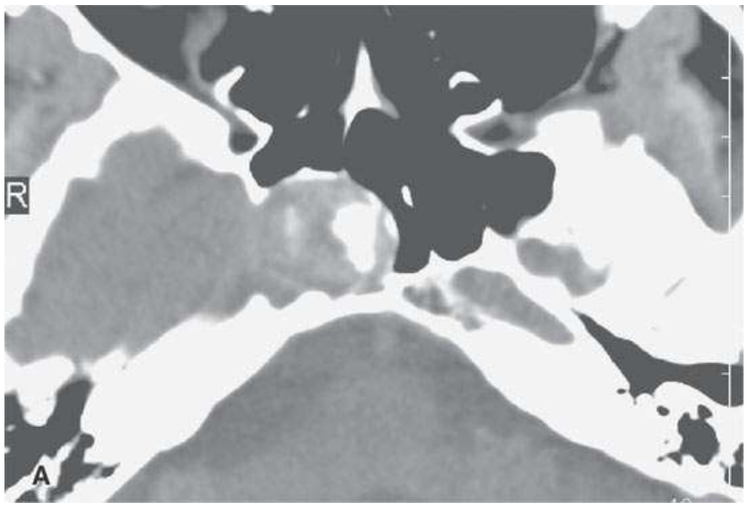

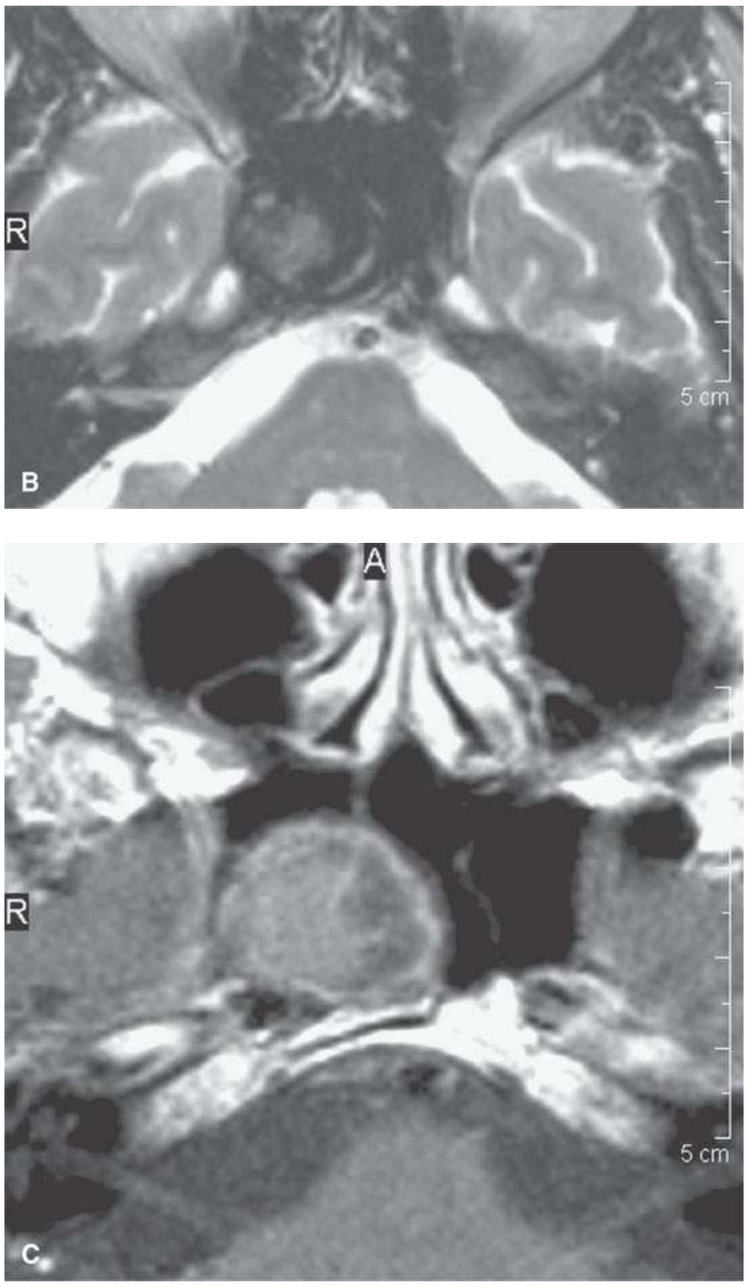

FIGURE 12.7. Cavernous segment aneurysm. The calcification suggesting wall and mural thrombus calcification is obvious on computed tomography. On the magnetic resonance imaging in **(B)** and **(C)**, the findings are more ambiguous.

CALCIFICATION AS SEEN ON COMPUTED TOMOGRAPHY AND MAGNETIC RESONANCE IMAGING

Calcification and ossification are often very difficult to recognize on MR studies as such, but calcification can be anticipated in certain situations. A focal or diffuse area of markedly diminished signal intensity or signal void on all pulse sequences suggests calcification, ossification, fibrosis, or very chronic blood products (Fig. 12.8). Other possible explanations for such decreased signal include flow void, air, surgical clip, foreign body (Figs. 12.6 and 12.9), or other very proton poor substance or at least something lacking enough mobile protons to create a signal (Fig. 12.10). Small foci of calcification or ossification (several millimeters) are very likely to go unnoticed on standard spin echo (SE) sequences depending on the nature of the surrounding tissues. Gradient echo techniques can improve the rate of detection, or at least suspicion, of calcifications since these sequences are highly sensitive to the local field distortions produced by calcium-related susceptibility effects (Fig. 12.11 and Chapter 2). Gradient echo and susceptibility-weighted sequences are useful in the brain for this purpose, but their value is sometimes limited in the extracranial head and neck because these sequences are more prone to magnetic susceptibility artifacts that variably degrades image quality outside the brain depending on the adjacent anatomy and its vulnerability to susceptibility artifacts such as a mandible full of metal due to dental appliances.

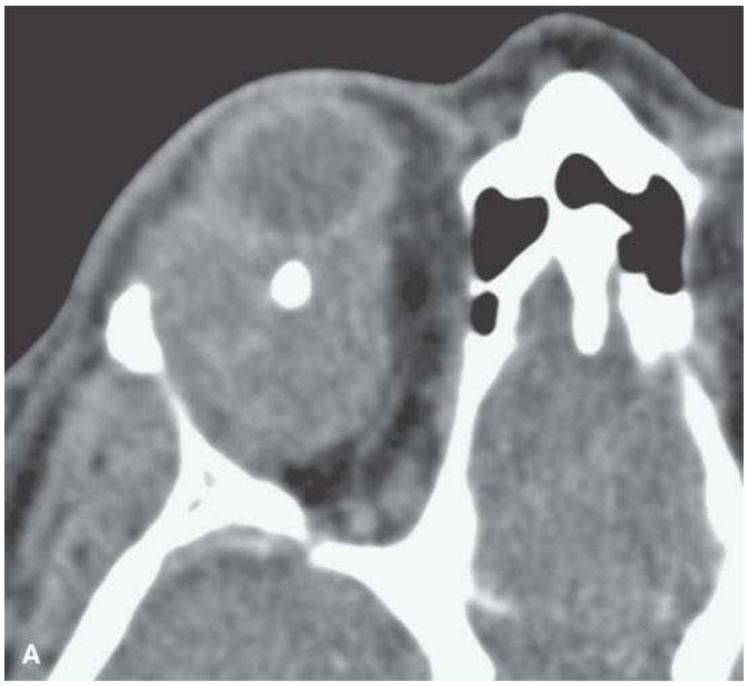

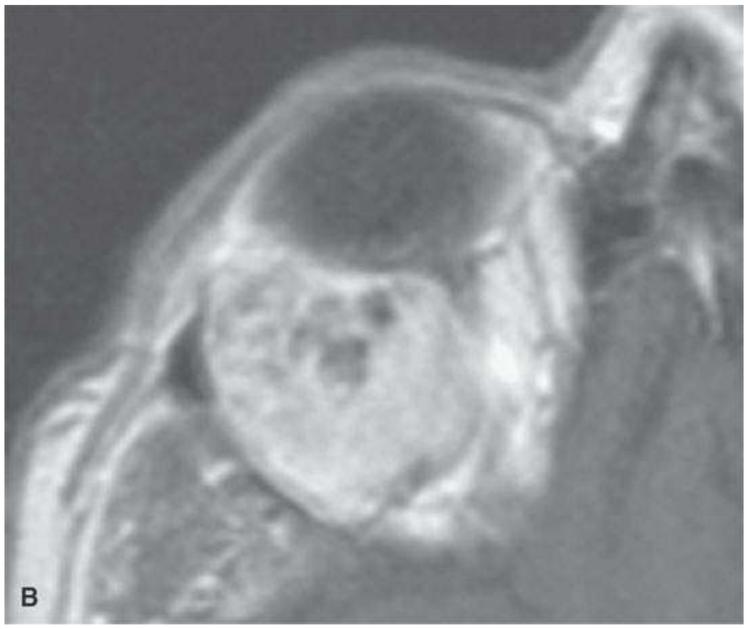

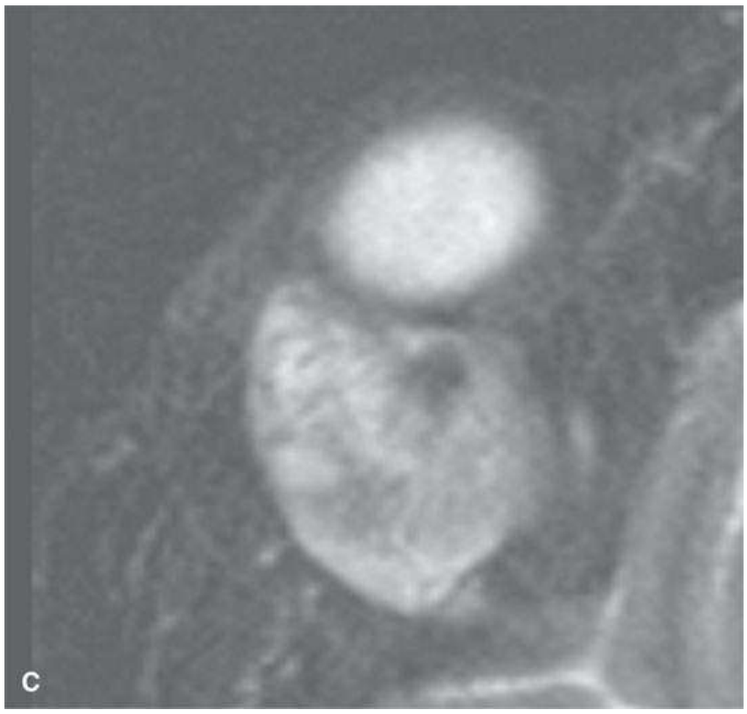

FIGURE 12.8. Adenoid cystic carcinoma of the lacrimal gland with possible calcification in impacted mucoid material or dystrophic calcification**.** The nature of the signal void is less clear on the contrast-enhanced T1-weighted magnetic resonance imaging (MRI) in **(B)** and the T2-weighted MRI in (C). In this case, the presence of a calcification adds nothing to the diagnostic process**.**

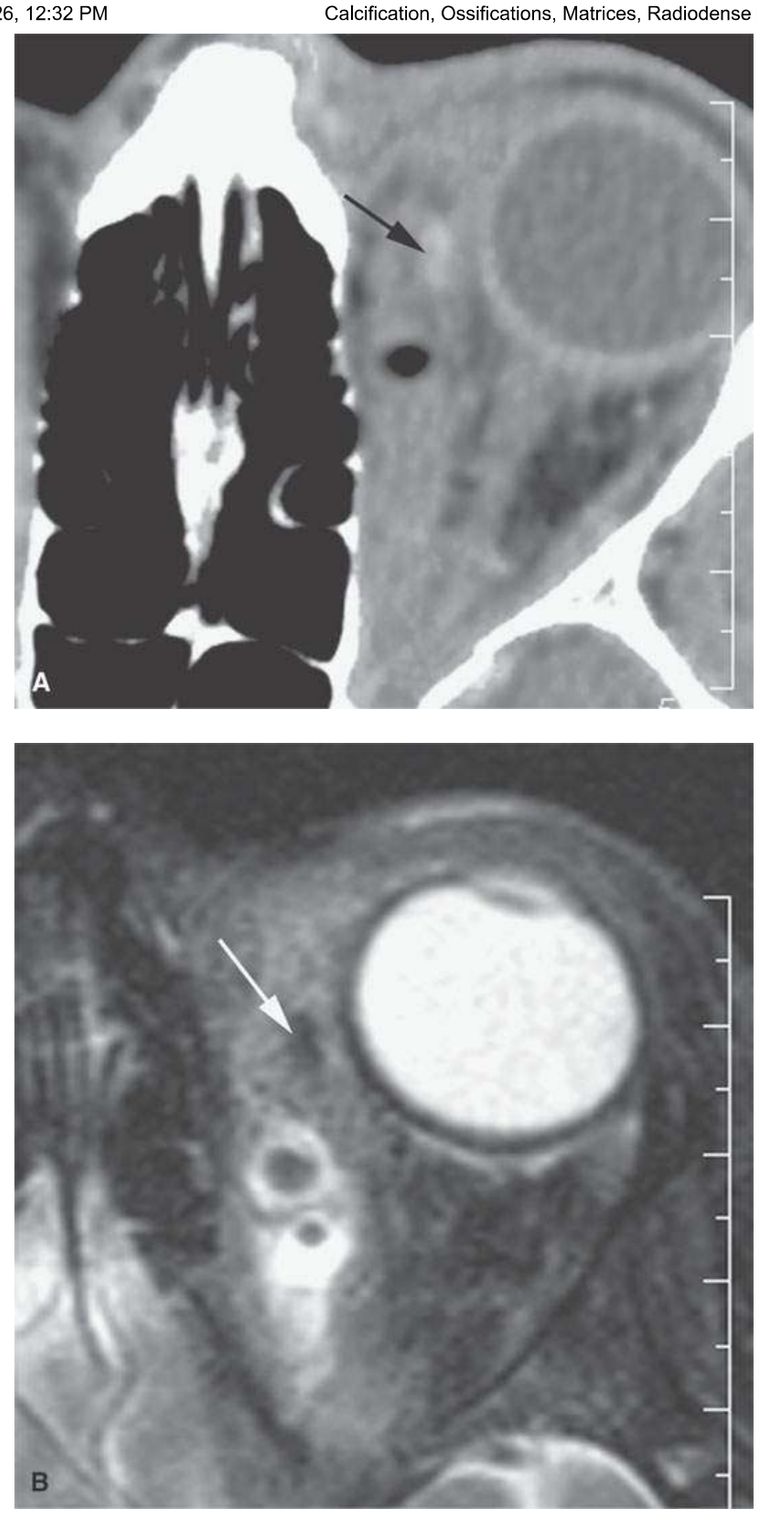

FIGURE 12.9. Penetrating orbital trauma**. A:The** wood fragment *(arrow)* is the same density as expected from calcification seen in the non–contrast-enhanced CT**.** Note the gas**. B:** In the T2-weighted magnetic resonance imaging, both the foreign body *(arrow)* and gas show as signal voids an obviously more ambiguous and less helpful scenario than with CT**.**

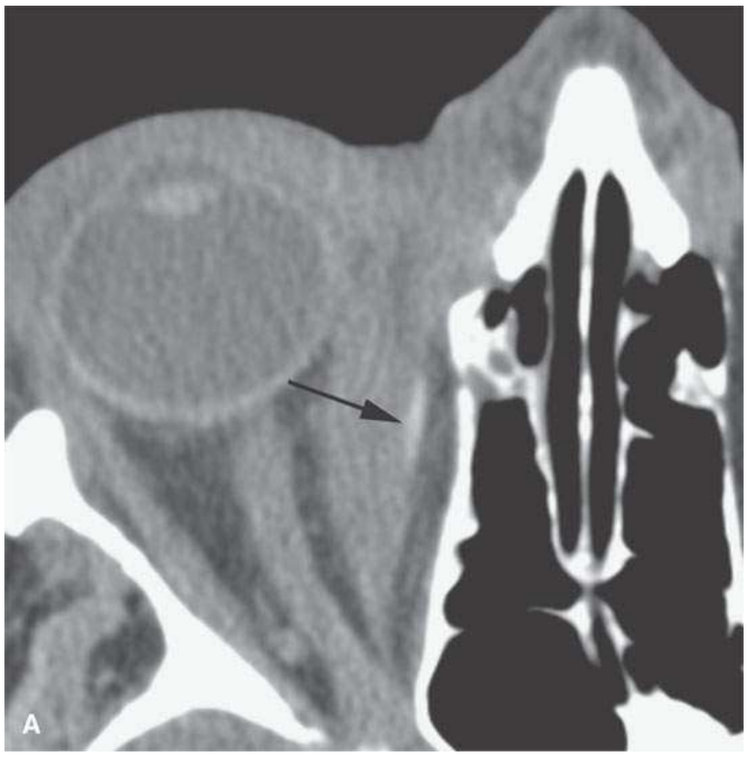
A

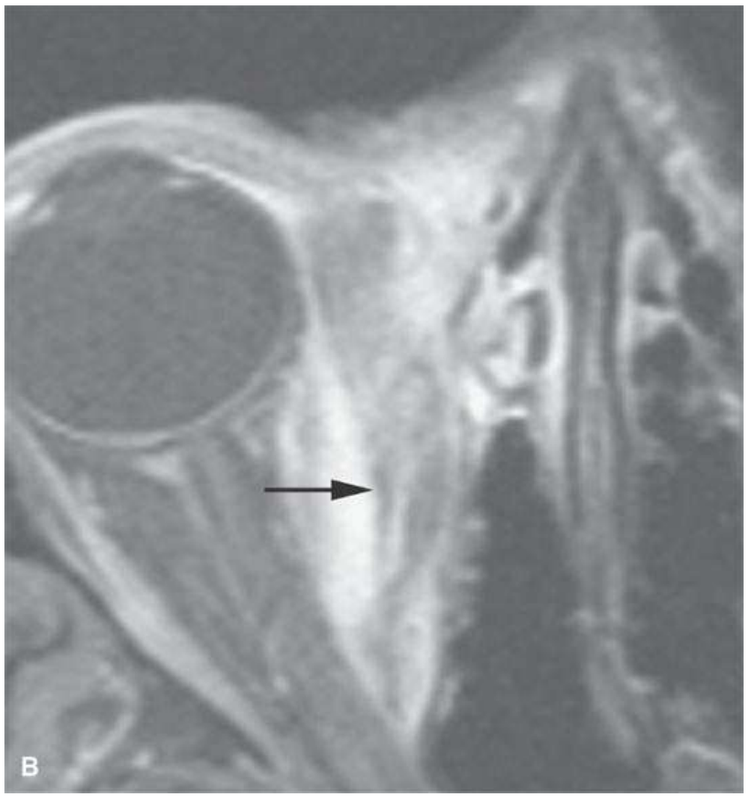
B

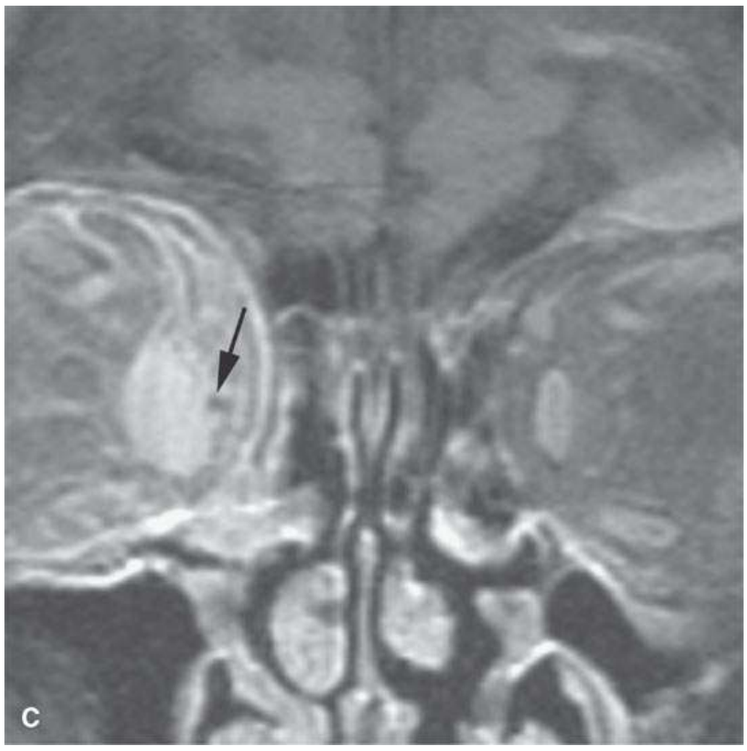

FIGURE 12.10. Penetrating plant material mimics a calcified foreign body on the computed tomography in (A). It is not really visible *(arrow)* on the fat-suppressed T1-weighted magnetic resonance imaging in **(B)**, but it can be seen *(arrow)* as a void on the coronal T2-weighted image in (C)**.**

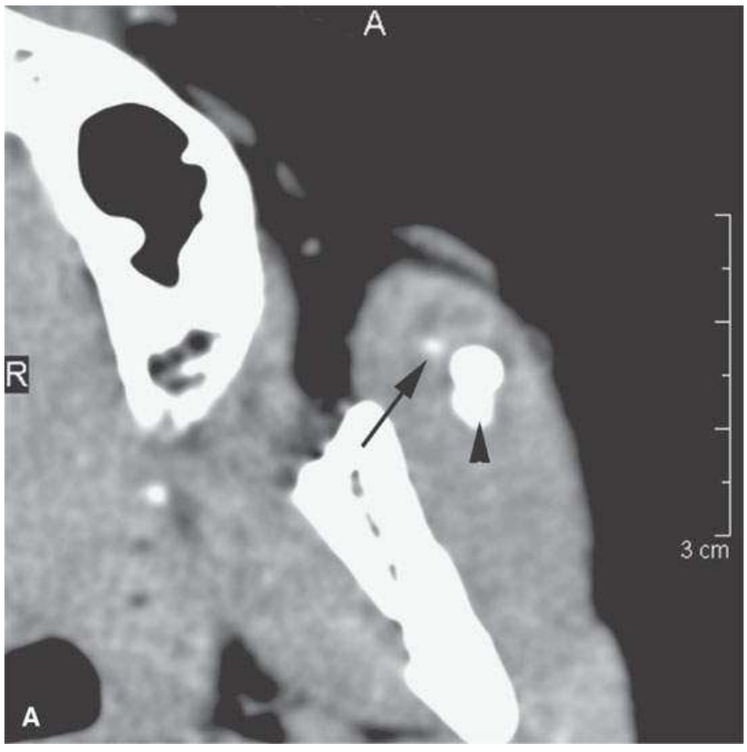

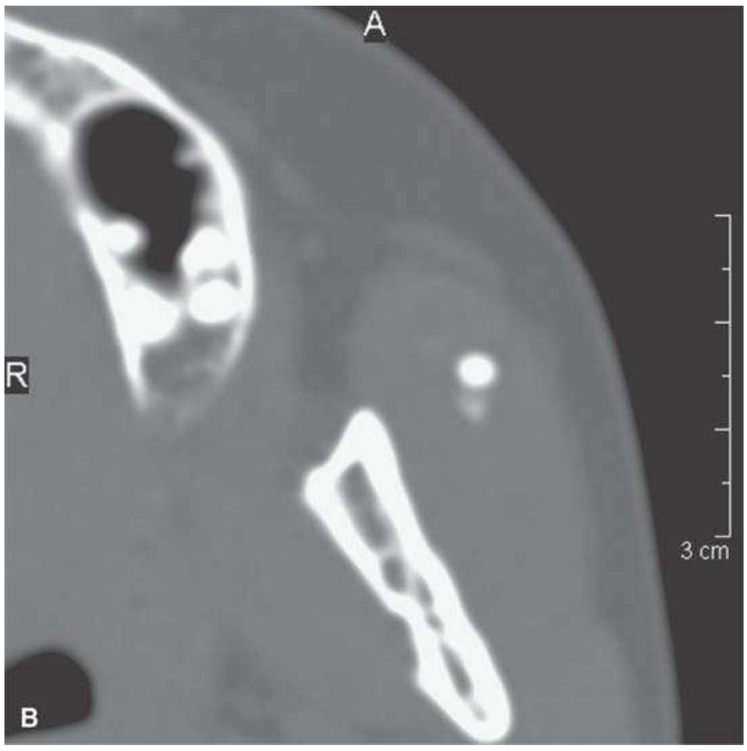
A
R
3 cm
B

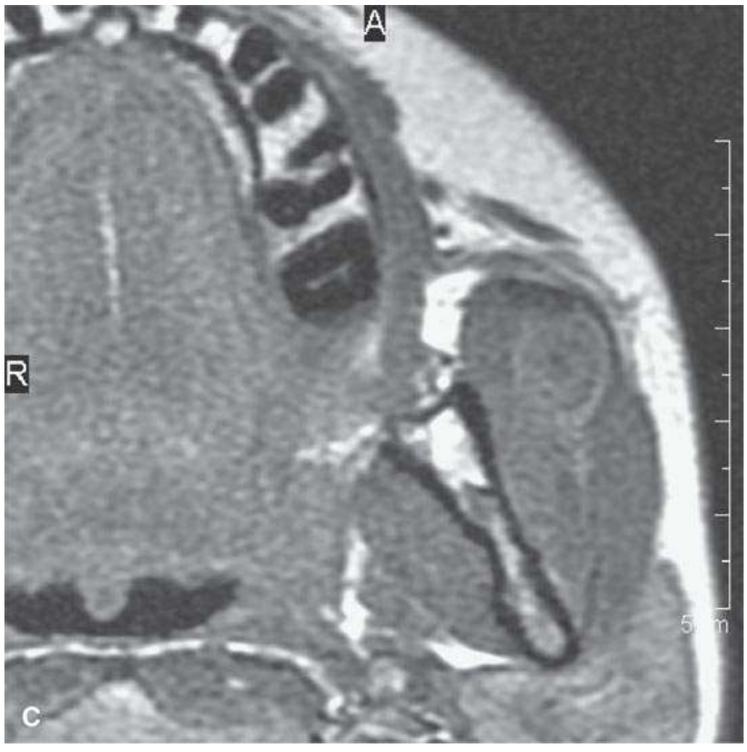
A
R
C

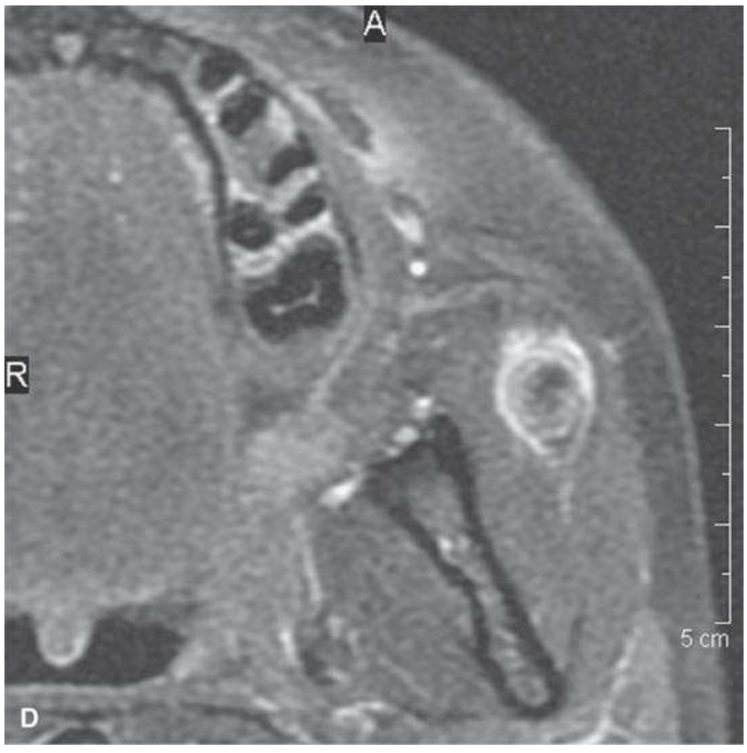
A
R
5 cm
D

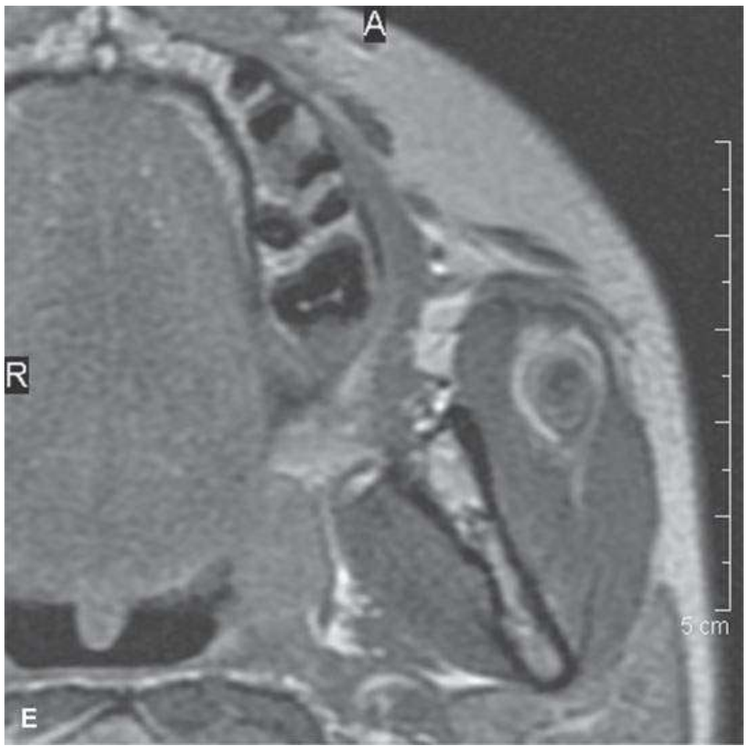
A
R
5 cm
E

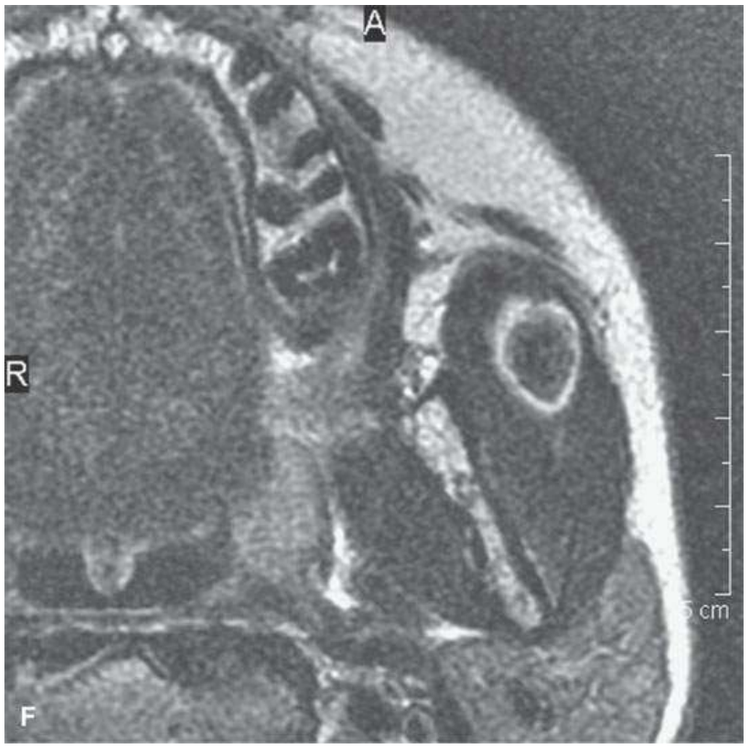
A
R
5 cm
F

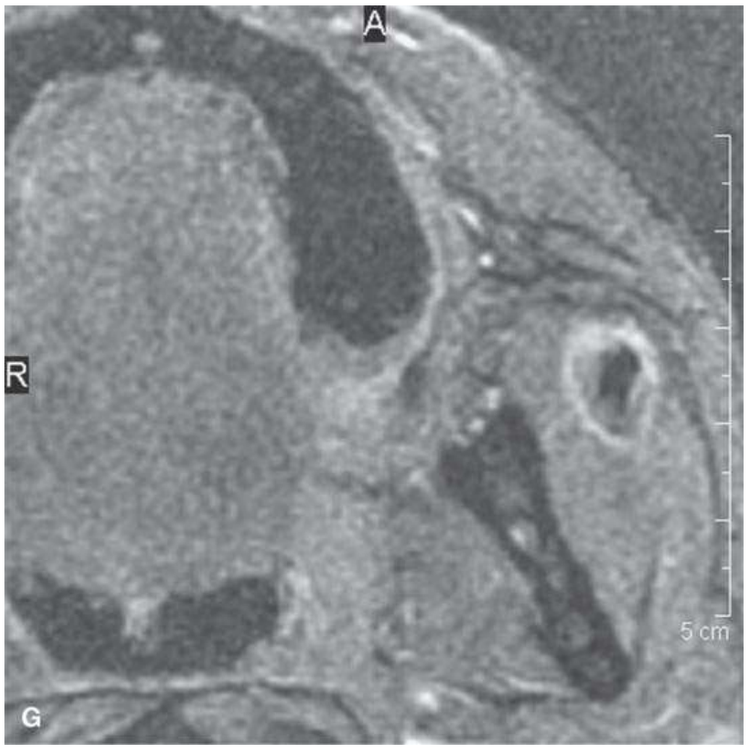
A
R
5 cm
G

FIGURE 12.11. Appearance of calcification on computed tomography (CT) and magnetic resonance imaging (MRI) in a small vascular malformation presenting as a cheek mass. The recognition of the calcification is useful in the differential diagnosis. Contrast-enhanced CT **(A)** shows enhancement *(arrow)* and the calcification (B). MRI including non–contrast-enhanced T1 weighted **(C)**, contrast-enhanced fat-suppressed T1 weighted **(D)**, contrast-enhanced T1 weighted **(E)**, T2 weighted **(F)**, and gradient echo **(G)**, all showing the calcifications as some degree of a signal void with some recognizable field distortion in the calcification in **(F)** as a clue to is "metallic" nature.

If the diagnosis is already known, then the MR depiction of the process may be adequate or yield more information than the CT. However, whenever such suggestive areas of consistently diminished signal are present and the nature of the low-intensity area is important for treatment or diagnostic purposes, a CT should be done to clarify the situation (Fig. 12.12).

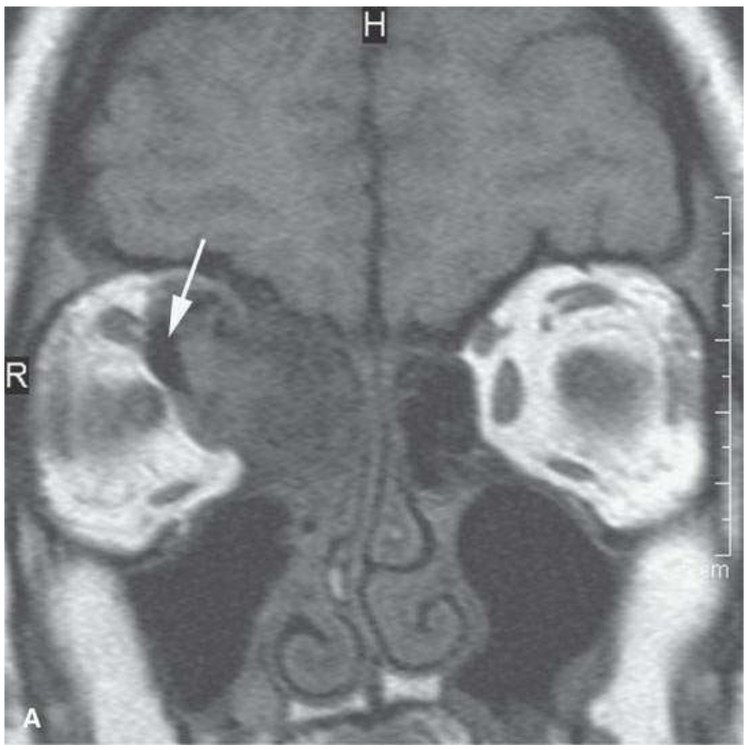

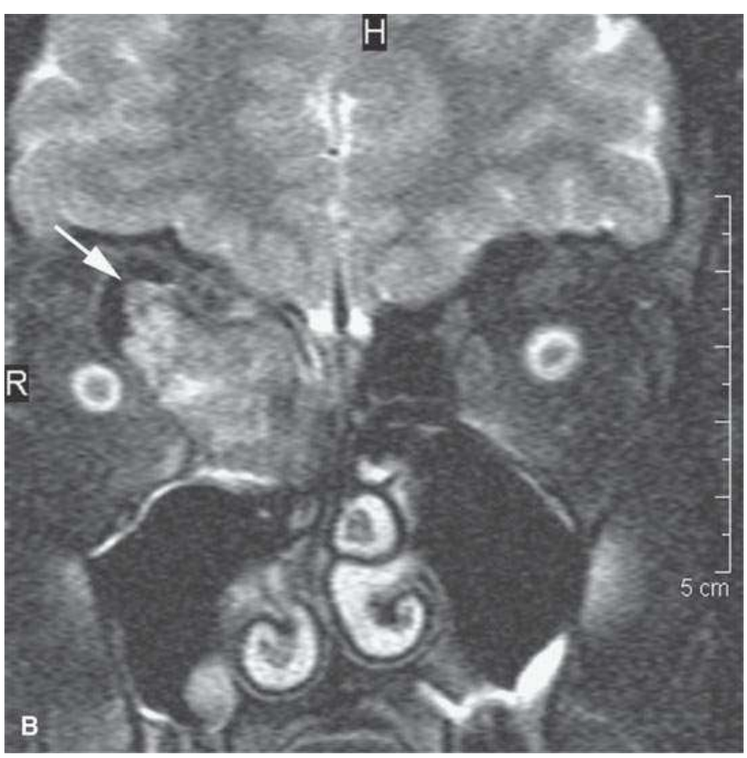

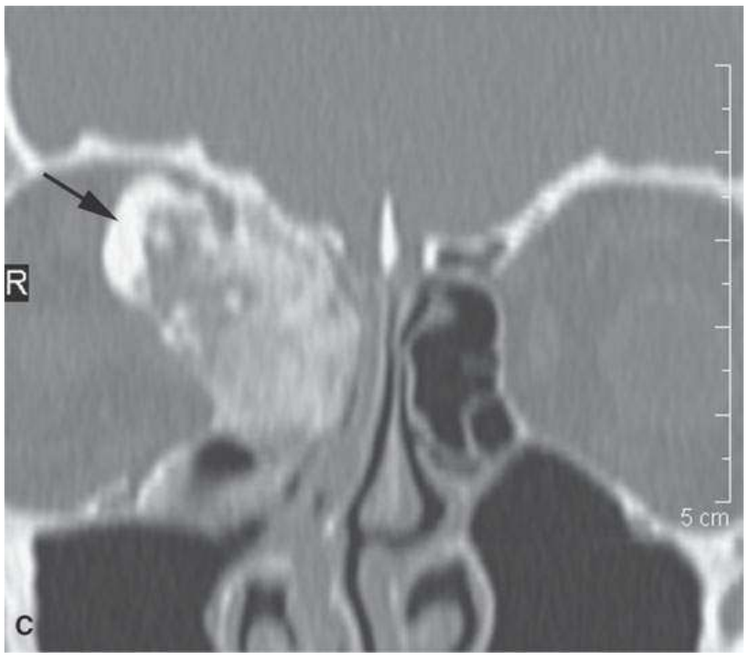

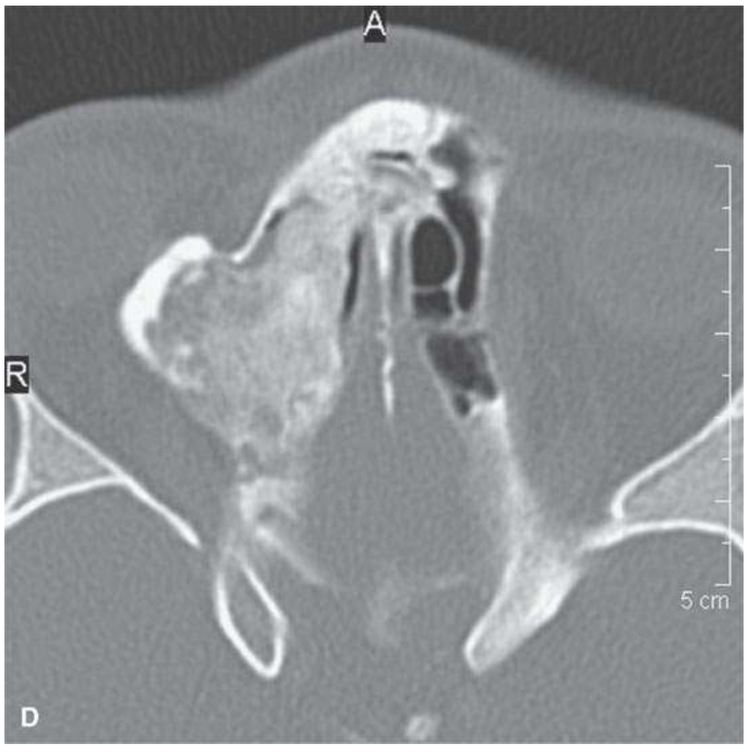

FIGURE 12.12. The obvious area of signal void is seen on the magnetic resonance images (T1-weighted non–contrast enhanced in **A** and T2 weighted in **B** by the *arrows*), but the nature of the remaining matrix and true nature of the signal void area is not clear *(arrow)* until viewing the non–contrast-enhanced computed tomography in **(C)** and (D)**.** This was diagnosed pathologically as an osteoma with elements of osteoblastoma**.**

Calcium may also be the cause of areas of increased signal intensity on T1-weighted images**.** This has been observed in patients with neurofibromatosis as areas of increased signal intensity in the basal ganglia (Fig. 12.13)**.**2 One group2has demonstrated that the effect is probably related to the physical state of the calcium in these regional areas of disordered brain maturation and thus altered MR signal. A similar situation may exist in calcium in solution in a fluid collection**.**

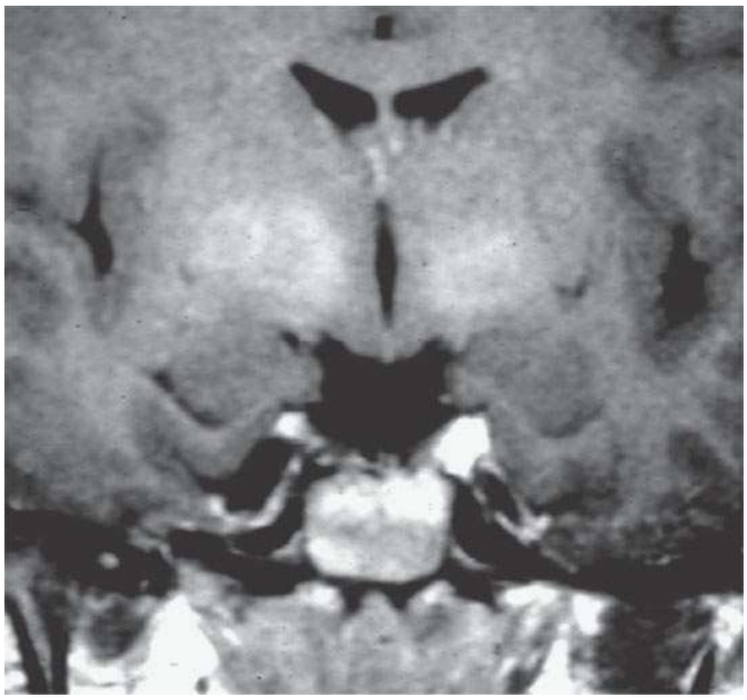

FIGURE 12.13. TI-weighted magnetic resonance showing high-attenuation areas in the globus pallidus in a patient with neurofibromatosis type I.

In general, the calcifications and areas of ossification on CT and plain films are very easily recognized as areas of discreet increased density with a morphology conforming to the source of their origin (Figs. 12.14 and 12.15). Occasionally, they may be confused with retained noncalcific foreign bodies, acute blood products, desiccated impacted secretions, or focal contrast enhancement (Fig. 12.16 compared to 12.5). If important to diagnosis, pre- and postcontrast CT images may be necessary. Currently, this is not a routine in any CT protocol except the initial evaluation of a potential retinoblastoma.

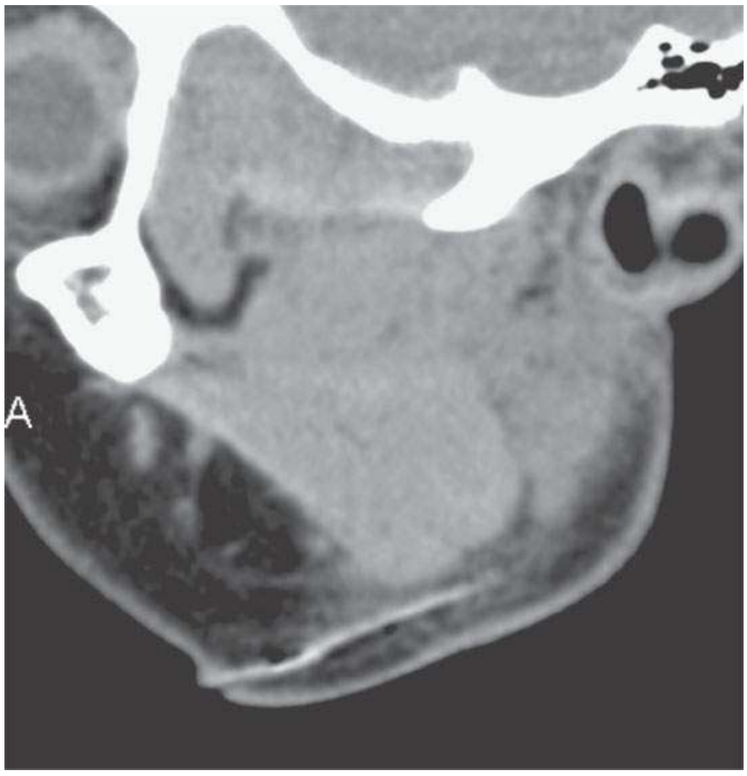

FIGURE 12.14. Contrast-enhanced computed tomography that shows a penetrating pine needle that likely would not have been visible on magnetic resonance imaging. The morphology is the clue to the nature of the material; in this situation, its density is not helpful.

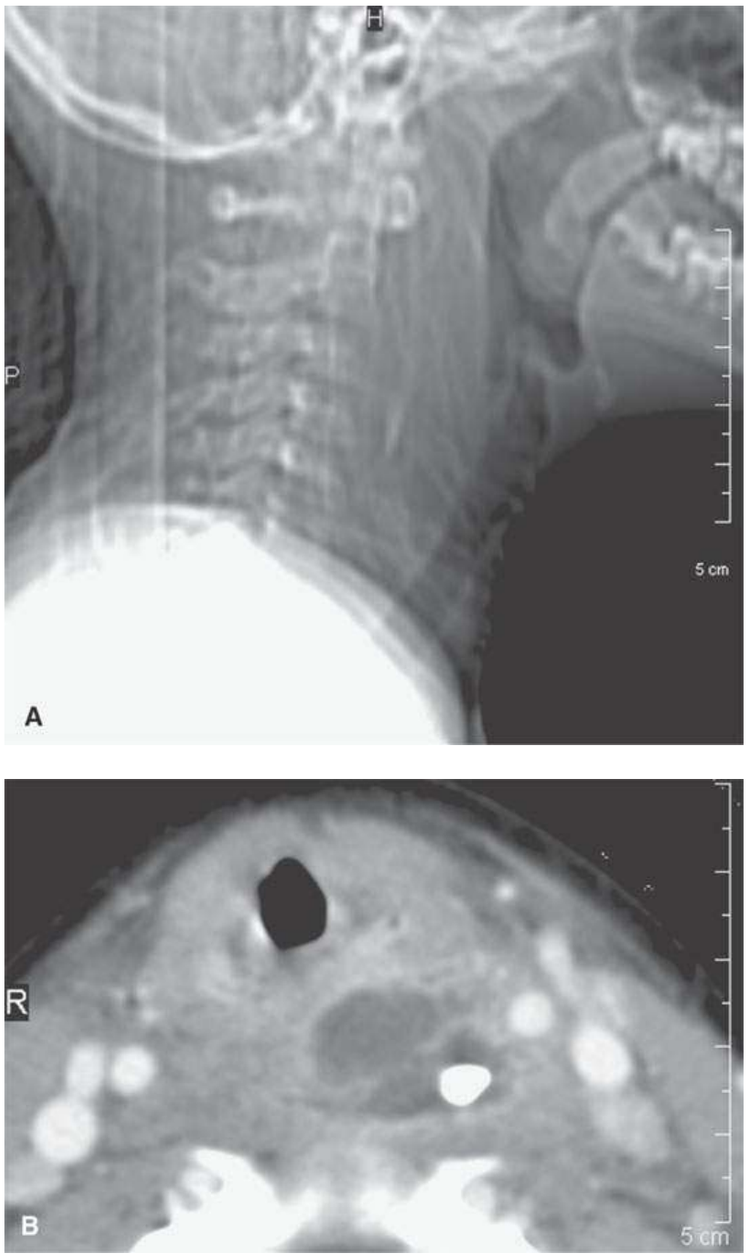

FIGURE 12.15. The calcified penetrating chicken bone fragment is seen both on the plain film **(A)** and in the middle of the abscess as seen on computed tomography (B). The diagnosis is much more straightforward than would be possible on magnetic resonance imaging.

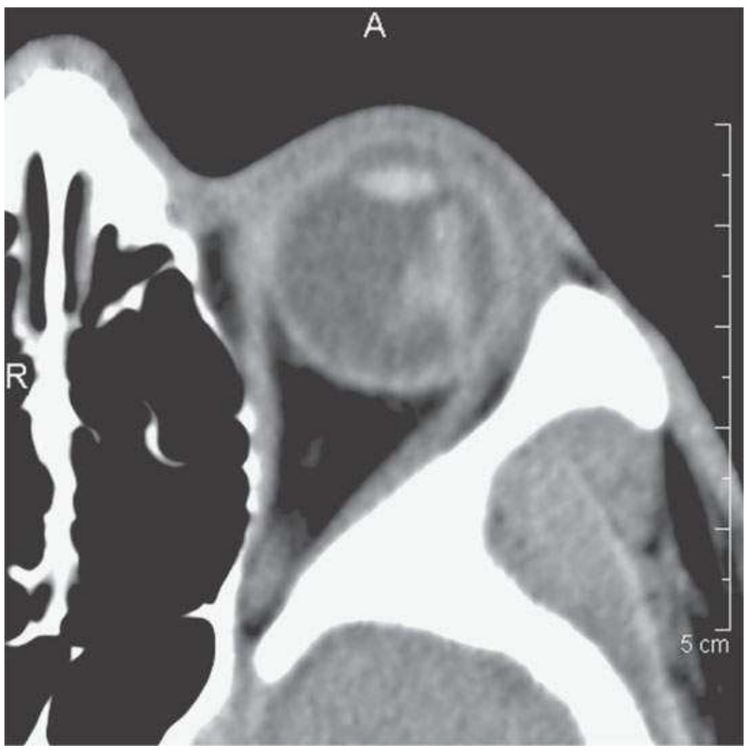

FIGURE 12.16. Computed tomography of a foreign body with a calcium-equivalent density that was mistaken originally for a vitreous hemorrhage. The "geometric morphology" is a clue to its origin outside the body, while the density is ambiguous. Compare this figure with Figure 12.5.

The exact morphology of calcification and ossification varies considerably with its origin. The morphology of calcification as seen on CT and plain films and MRI in various pathologic conditions are summarized in the following material and then described more specifically as they are associated with normal anatomic variations and pathologic conditions at various specific anatomic sites of origin (Fig. 12.6B–E).

PHYSIOLOGIC CALCIFICATIONS

Physiologic calcifications are generally related to the maturation and aging process in tissues.[3] As such, most have a tendency to be more prevalent with aging. Physiologic calcification is probably best known to occur intracranially, such as those of the pineal, dural, and choroid.[3] The globus pallidus is the most common calcified intra-axial structure.[3]

Physiologic calcifications are most prevalent in the extracranial soft tissues of the head and upper neck in the stylohyoid ligament and cartilages of the external ear and its cartilaginous canal (Fig. 12.1). In the mid to lower neck, calcification of the laryngeal cartilages is highly variable, and this physiologic variation contributes to significant difficulty in recognizing cartilage abnormalities in very young patients and in patients at risk for cancer invasion of the laryngeal skeleton. The elastic cartilage of the epiglottis is not supposed to calcify. In fact, it does calcify (Fig. 12.17) occasionally. Tracheal cartilage calcification is also common but can also be a pathologic feature in tracheal pathology (Fig. 12.18).[4]

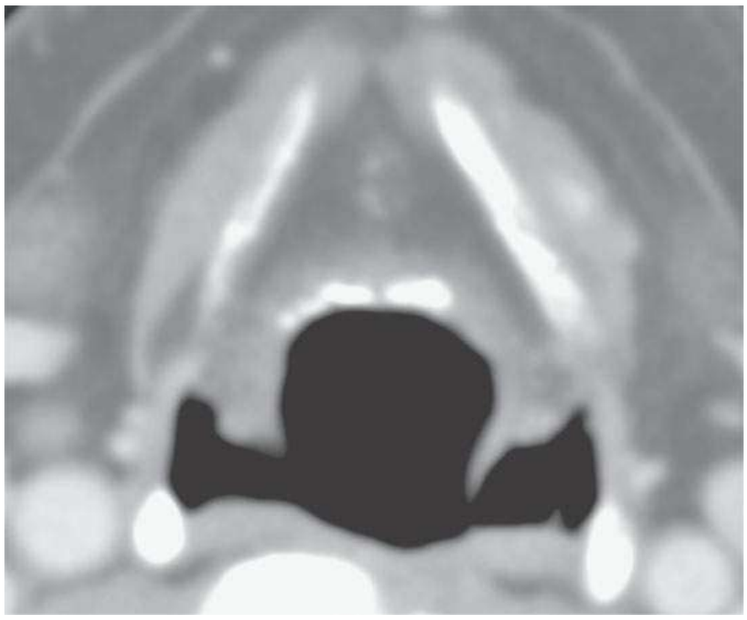

FIGURE 12.17. Computed tomography of "physiologic" calcification of the infrahyoid epiglottis. This is inconsequential.

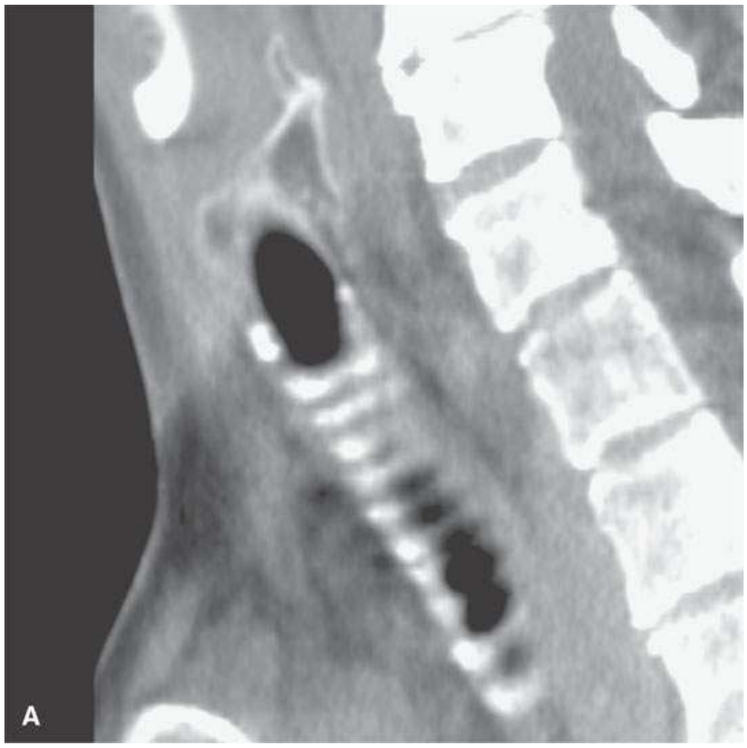

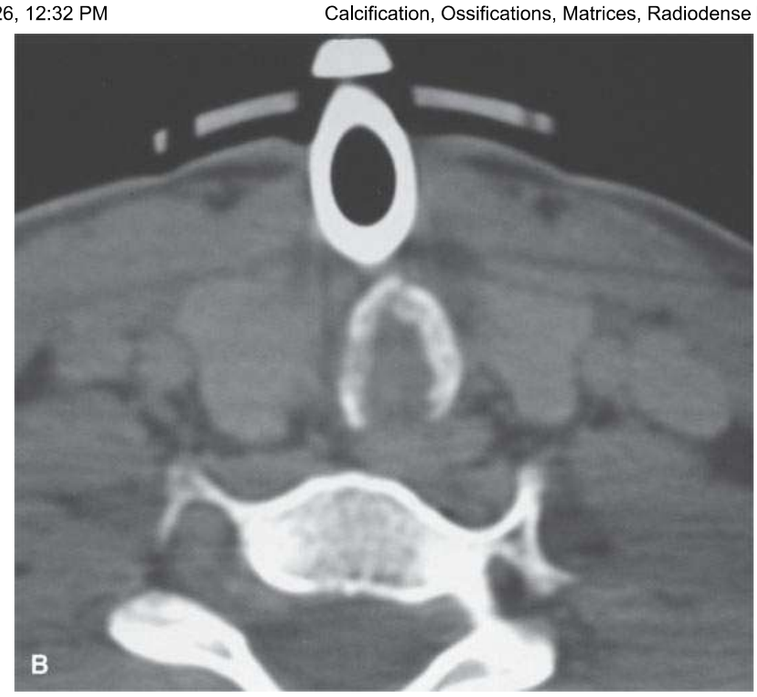

FIGURE 12.18. Computed tomography of physiologic tracheal calcification in **(A)** and dystrophic calcification in chondritis with chondromalacia of the trachea in (B).

DYSTROPHIC CALCIFICATION

Dystrophic calcification is one of the most common causes of nonphysiologic calcification seen in the extracranial head and neck. Dystrophic calcification is a final common pathway of tissue response seen in areas of tissue inflammation and necrosis due to infection, leftover blood products, tumor, or trauma. The specific appearance on imaging studies varies with the site, amount, and etiology of the tissue response.

Dystrophic calcification can be a useful source of information for medical decision making. Such usefulness occurs in patients with residual cervical metastatic nodes due to squamous cell carcinoma (SCCA) following radiotherapy, where focal calcification predicts a high risk of persistent viable tumor (Fig. 12.19).[5] However, dense keratin debris can mimic such dystrophic calcification in nodes involved with SCCA either before but more typically after radiotherapy (Fig. 12.4B). Other treated cancer in nodes can become dystrophic and calcify (Fig. 12.20). Nonmalignant lymph node pathologies can also result in dystrophic, end-stage calcification (Fig. 12.21). In most cases, such information is useful but often in itself not definitive with regard to medical decision making.

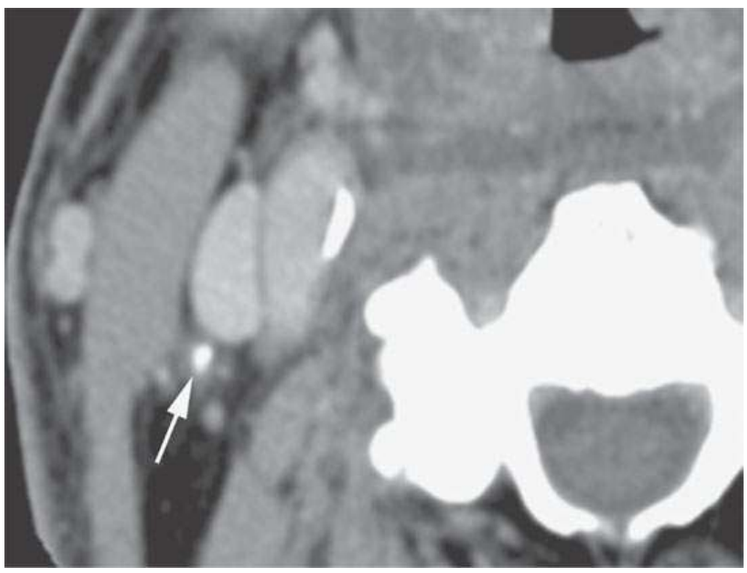

FIGURE 12.19. Computed tomography of surgically proven dystrophic calcification in a metastatic cervical lymph node containing residual cancer following radiotherapy.

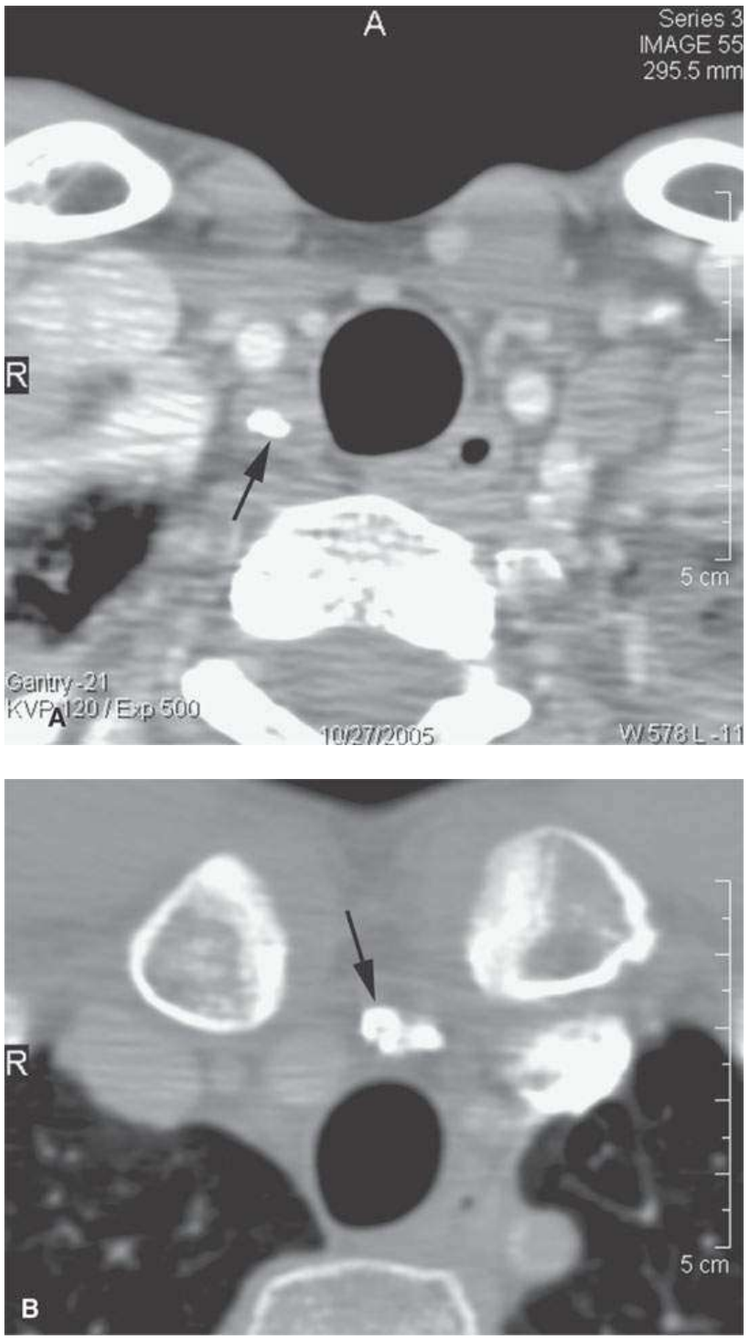

FIGURE 12.20. Computed tomography of dystrophically calcified level 6 nodes *(arrows)* following treatment for lymphoma.

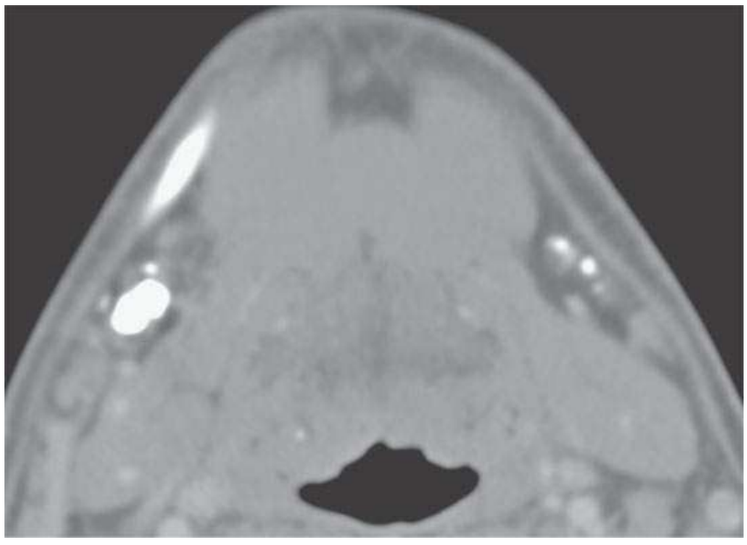

FIGURE 12.21. Computed tomography of calcified level 1 nodes of uncertain cause but nonneoplastic and probably inflammatory etiology.

Vascular calcification due to atherosclerotic disease is likely the most common nonphysiologic calcification seen in adult head and neck region CT (Fig. 12.22).6 This is probably something that probably receives only a passing amount of attention on head and neck studies done for other reasons. Atherosclerotic vascular calcification should be considered a form of dystrophic calcification in areas of plaque inflammation and prior hemorrhage.6 This is usually not a finding of tremendous importance; however, finding rimlike calcification in a mass may be critical to the recognition of that mass as being an aneurysm (Figs. 12.7, 7.12, and 23.12). Recognition of more routine plaques, usually at the carotid bifurcation, may also lead to a diagnosis of otherwise unknown critical flow-limiting brachiocephalic vessel occlusive changes.

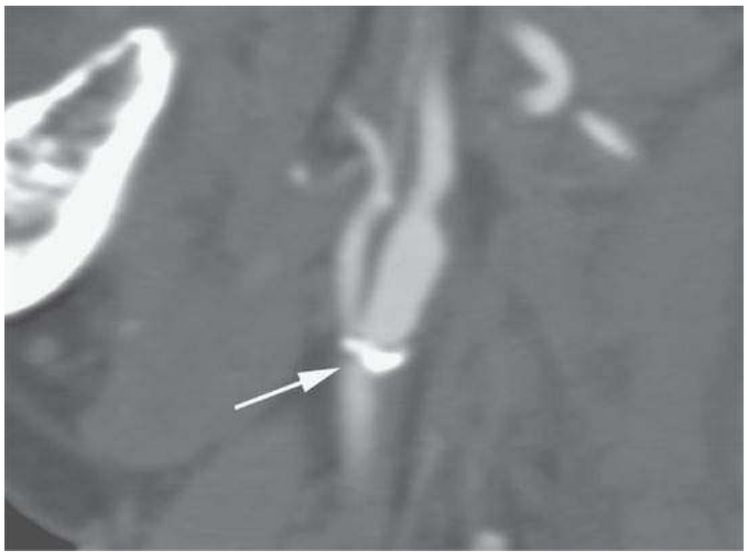

FIGURE 12.22. Computed tomography of a carotid bifurcation calcification *(arrow)*, showing an obvious strength of computed tomographic angiography over magnetic resonance angiography and vascular ultrasound.

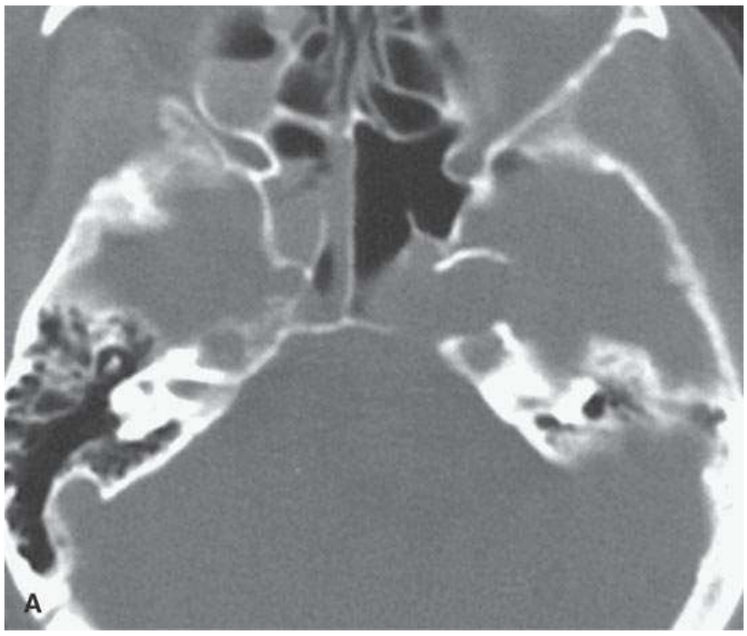

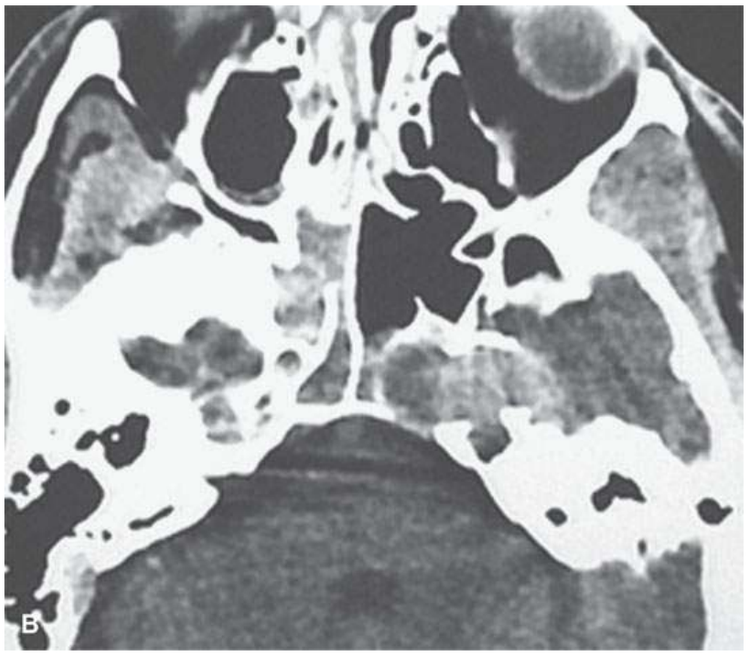

FIGURE 12.23. Computed tomography of the petrous apex and aneurysm, wherein recognizing calcification is critical to proper diagnostic decision making.

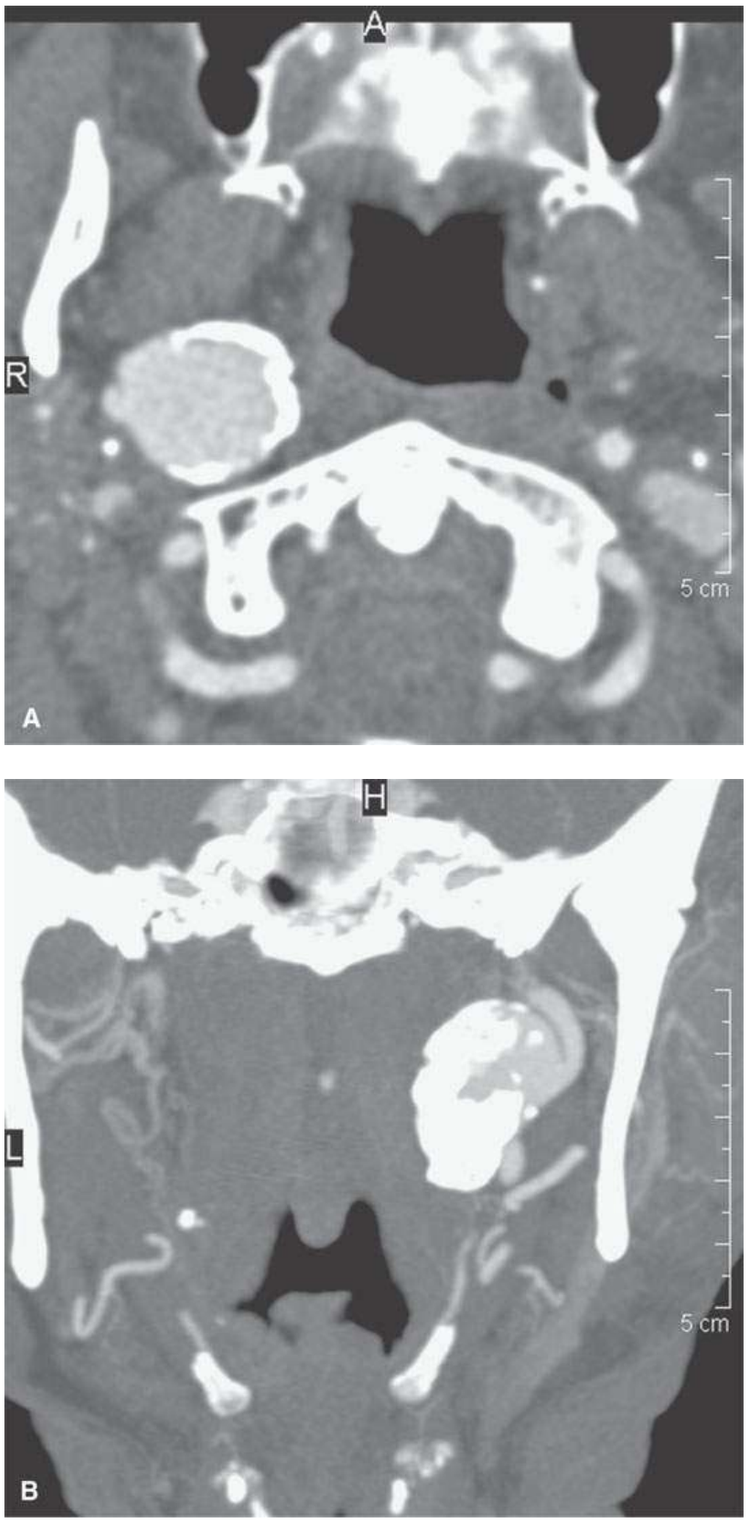

FIGURE 12.24. Computed tomography of the upper cervical carotid and parapharyngeal space aneurysm, wherein recognizing calcification is critical to proper diagnostic decision making.

Punctate calcification in impacted sinus secretions that are colonized by fungi frequently leads to a specific diagnosis of chronic allergic (noninvasive) fungal sinusitis (Fig. 12.25).7 Linear dystrophic calcification in the sinus mucosa can be seen as a result of chronic mucosal inflammation (Fig. 12.26) and have no particular predictive value. Following dental or sinus operative procedures, retained foreign bodies can mimic calcification or themselves become calcified. Some of these may actually be originally calcific in nature, such as retained bone fragments or fragments of teeth (Fig. 12.27).

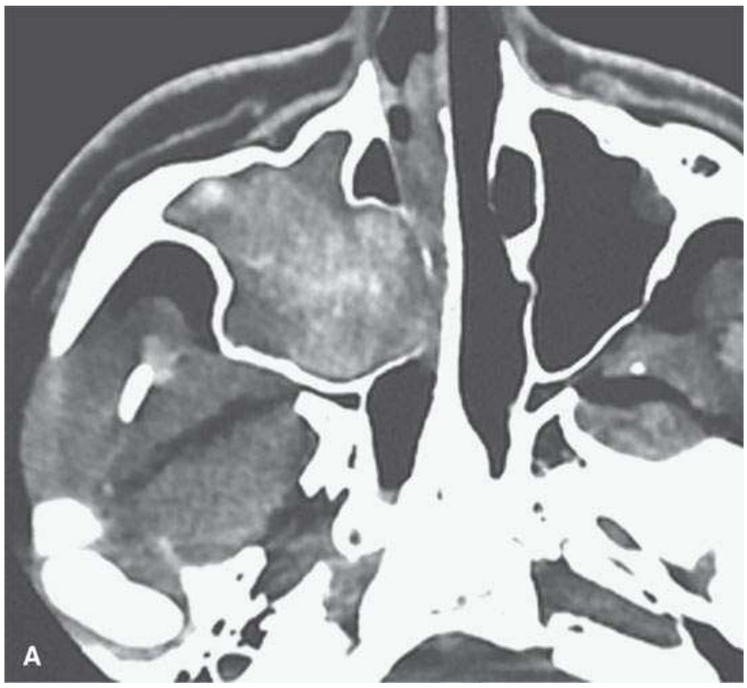
A

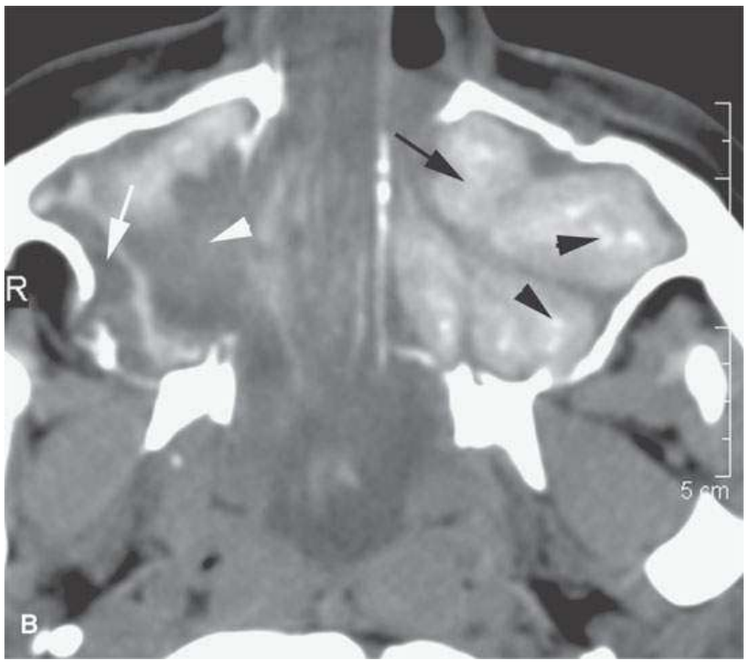
R
5 cm
B

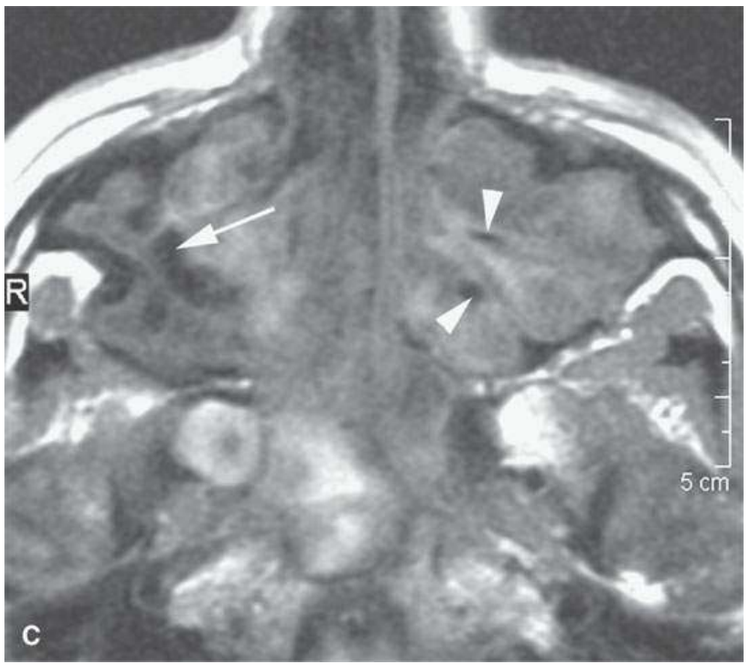
R
5 cm
C

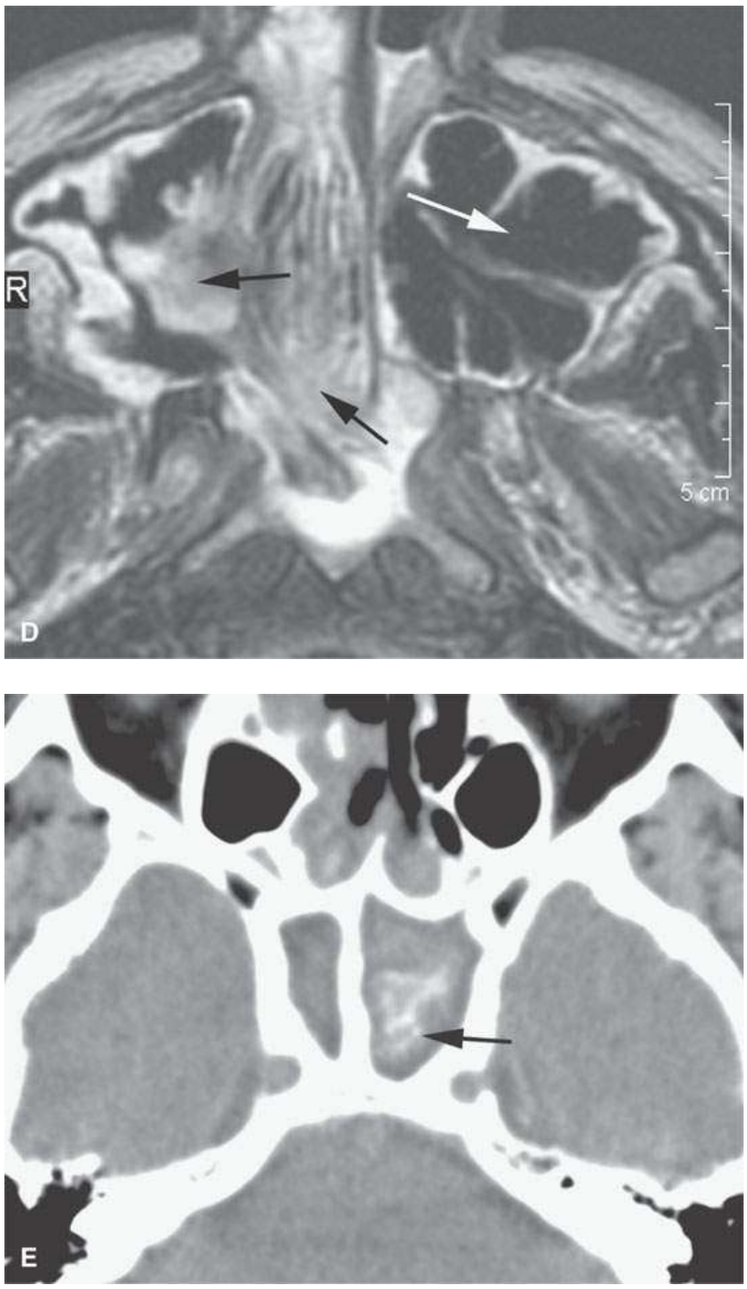

FIGURE 12.25. Sinus "calcifications." **A:** This was thought to be mucocele with allergic polyposis but turned out to be dystrophic mineralization and dense secretions in an inverted papilloma. **B–D:** Computed tomography showing fungal-related "calcification" *(arrowheads)* in a patient with chronic allergic fungal sinusitis and otherwise inherent density of the variously desiccated polyps *(arrows)*. The "calcifications" *(arrowheads)* and overall disease process present a less clear "gestalt" for this disease on magnetic resonance imaging (MRI) (T1-weighted non–contrast-enhanced in **C** and T2-weighted in **D**), although to one acquainted with this spectrum of findings, the diagnosis is relatively straightforward on MRI as well. When more localized, the magnetic resonance appearance can be mimicked by fibro-osseous lesions in particular but also other matrix-producing and otherwise fibrous lesions. **E:** Fairly typical "calcification" in fungal colonization of the left sphenoid sinus *(arrow)*.

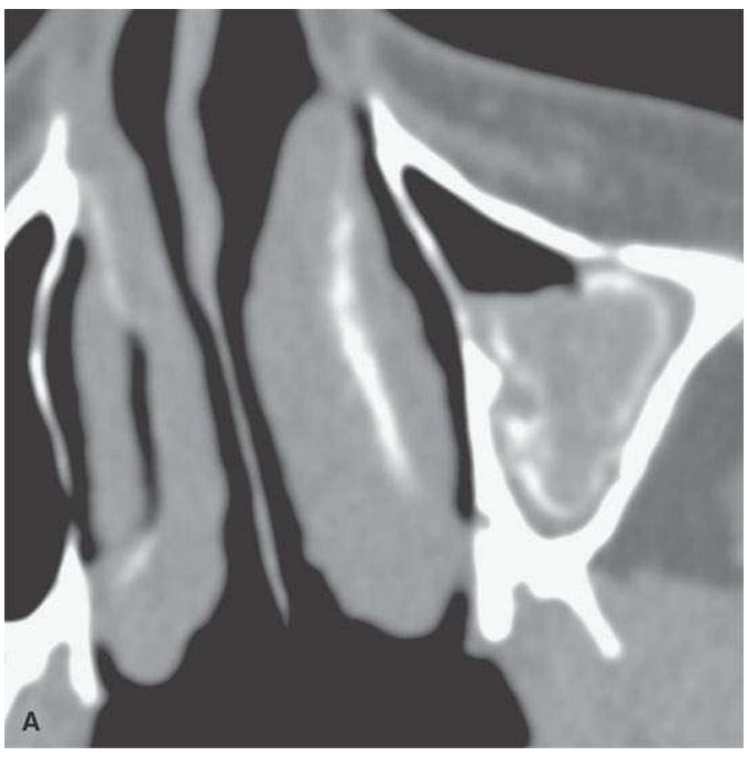

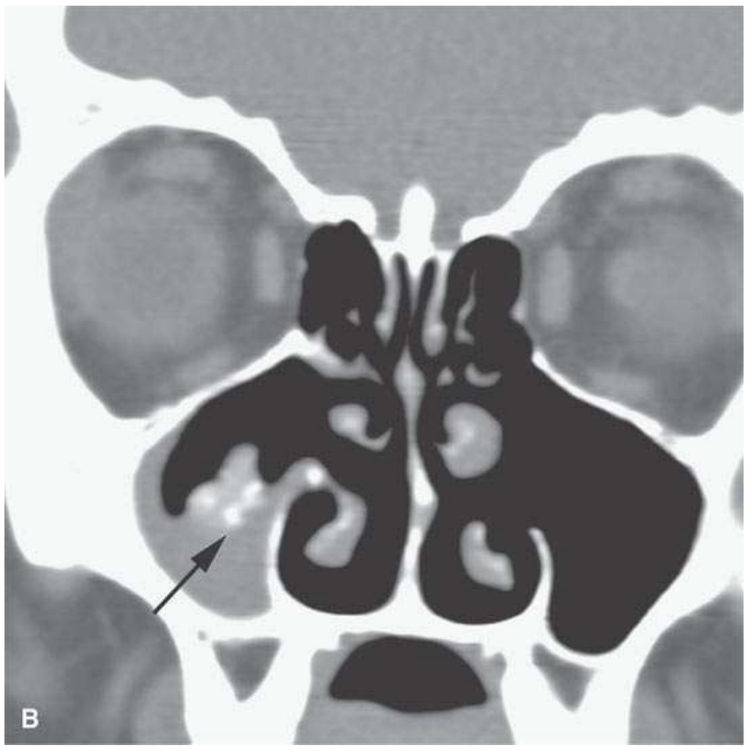
B

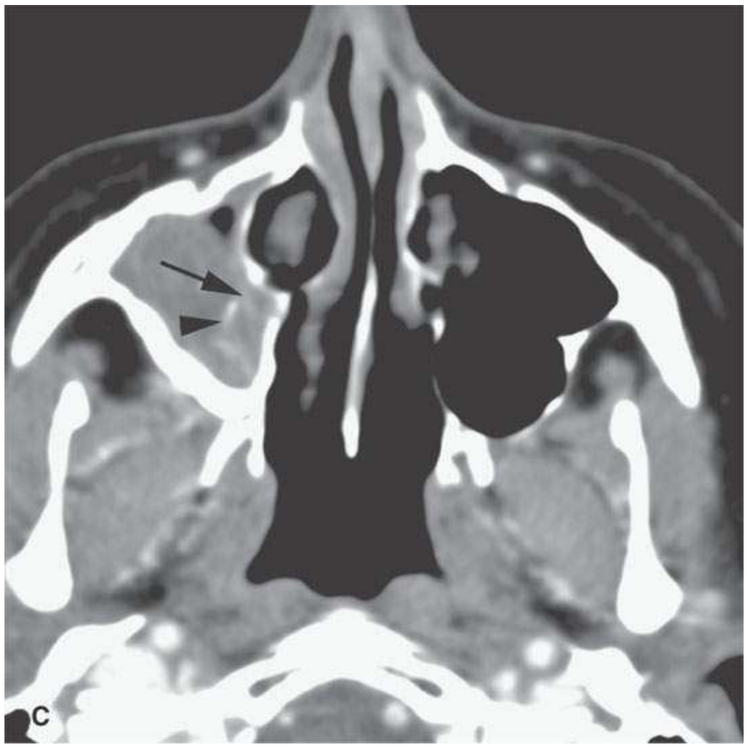
C

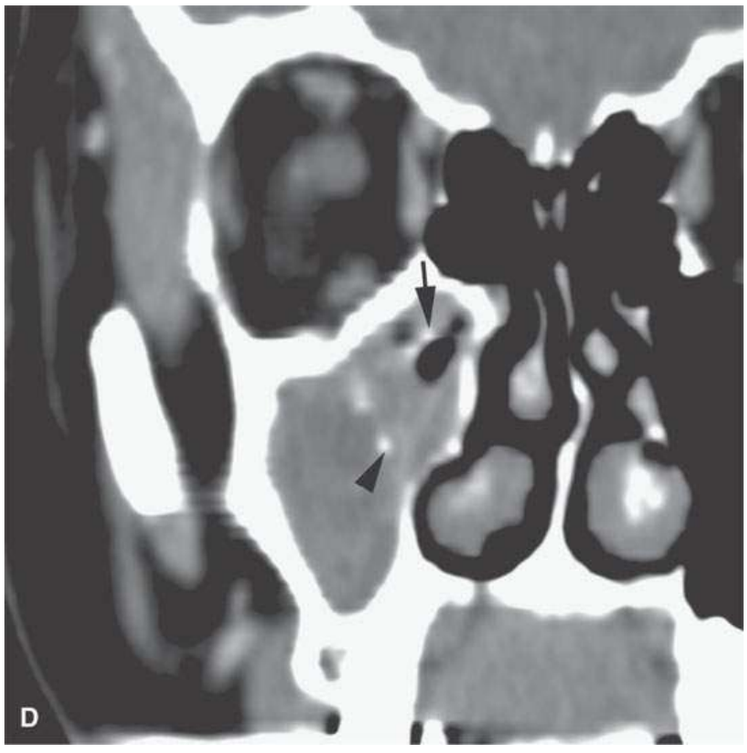
D

FIGURE 12.26. Sinus "calcifications" continued. **A:** Typical computed tomography (CT) pattern of dystrophic mucosal calcification. **B:** Relatively typical, proven CT fungal "calcification" pattern centrally within the luminal secretions *(arrow)*. **C, D:** More ambiguous pattern with *arrows* suggesting dystrophic mucosal "calcification" and *arrowheads* suggesting fungal calcification. No fungi were found at surgery.

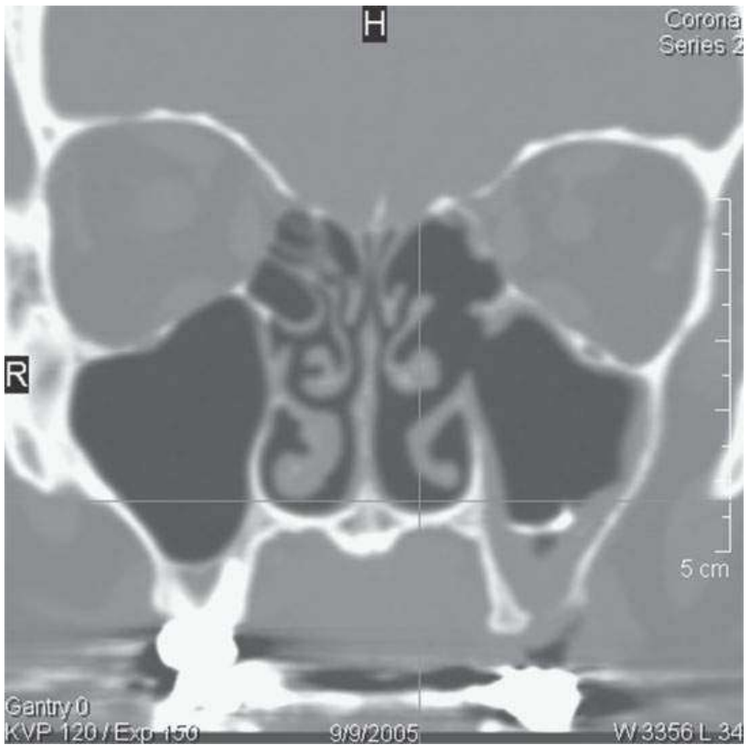

FIGURE 12.27. Partially calcific and partially metallic foreign body (surgically proven) following dental surgery that caused chronic recurrent disease.

Inconsequential dystrophic calcification frequently is seen in the palatine and lingual tonsils as the residual of prior infection or within retained food particles. Such calcific-appearing densities might actually be due to noncalcified impacted and desiccated secretions (Fig. 12.4A). Similar dystrophic "sclerotic" change can be seen in advanced cases of tympanosclerosis and be quite useful in anticipating just how difficult restorative surgery might be (Fig. 12.28). The aging sclera may show zones of dystrophic calcification.

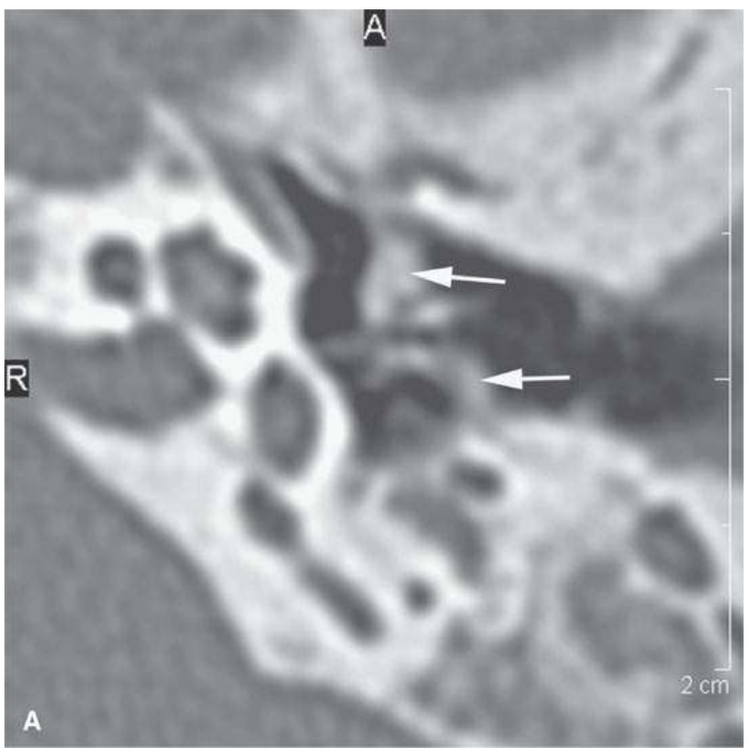

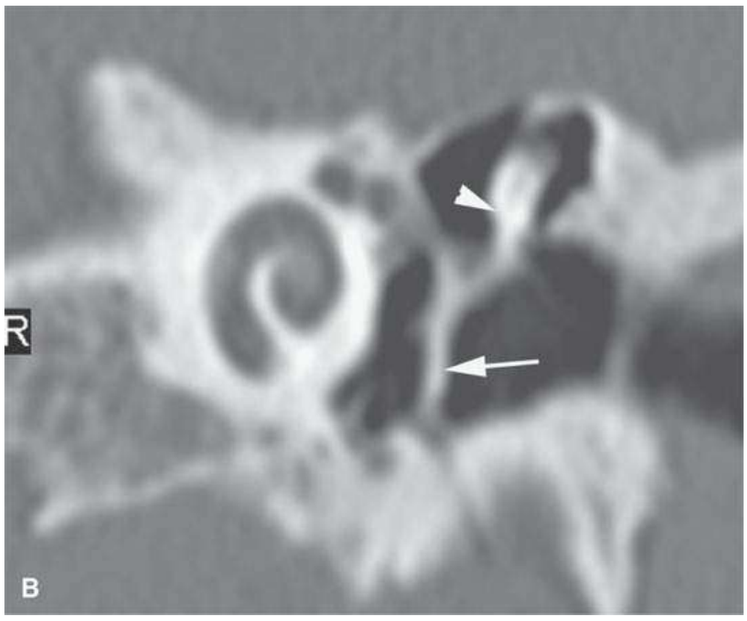

FIGURE 12.28. Computed tomography of the hyperdense mucosal changes of tympanosclerosis *(arrows)* that approach and in some areas match the visible density of the ossicles (*arrowhead* in **B**).

Dystrophic calcification may be seen as a regressive change within masses in areas of tumor necrosis or prior intratumoral hemorrhage. This may help in differential diagnosis or be of no particular value, and it can also be misleading (Figs. 12.2 and 12.29). This can be a mechanism of the calcification commonly present in thyroid nodules and lead to the formation of psammoma bodies, which are highly associated with thyroid malignancy (Fig. 12.30).[8,9] Such calcified regressive changes may be difficult to distinguish from calcification within the tumor matrix.

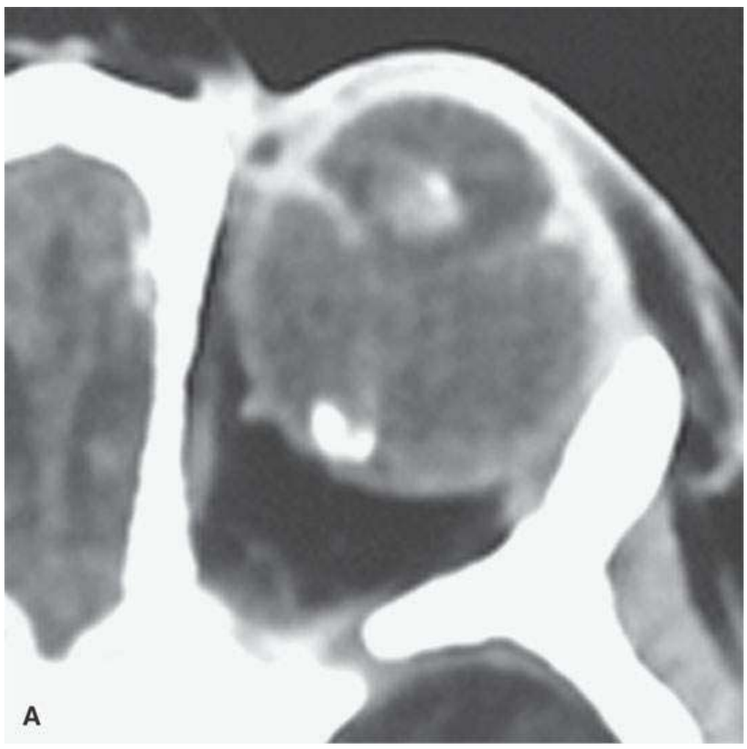

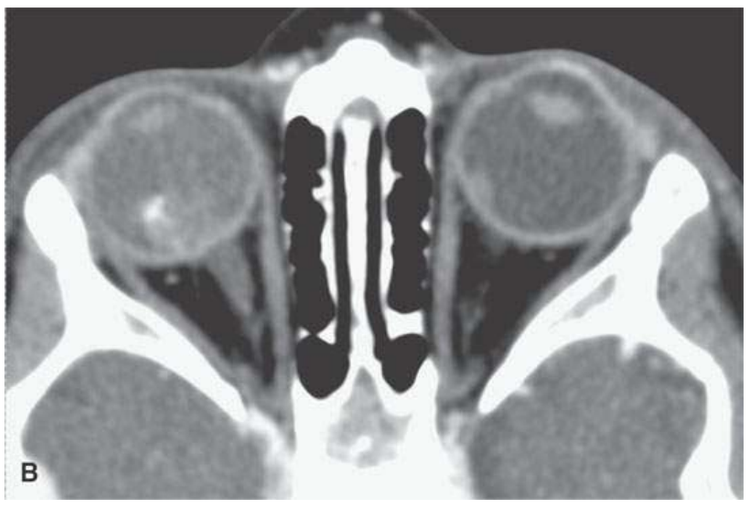

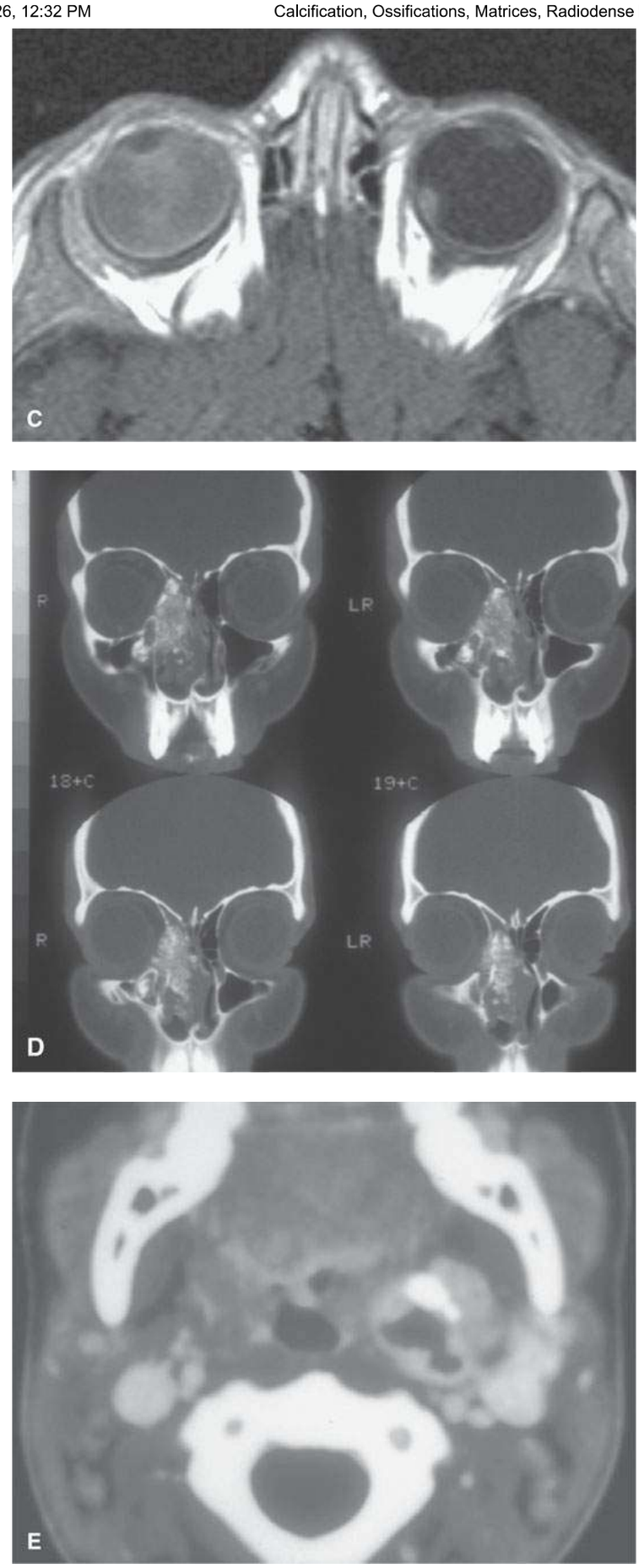

FIGURE 12.29. Useful, potentially misleading, and useless and potentially misleading patterns of calcification. The first two cases are useful. **A:** Contrast-enhanced computed tomography (CECT) of a child with leukocoria of uncertain etiology with an unmistakable calcified retinoblastoma confined to the globe as a cause of the leukocoria and complete retinal detachment. **B, C:** Another child with retinoblastoma bilaterally with the diagnosis much more obvious on the CECT in **(B)** than the T1-weighted contrast-enhanced magnetic resonance in (C). The following case is potentially misleading. **D:** CECT shows a nasal cavity olfactory neuroblastoma with extensive (atypical) calcification that might lead some down the wrong diagnostic pathway based on imaging, although biopsy is the prime determinant. The following case is useless and potentially misleading. **E:** Leiomyosarcoma of the prestyloid parapharyngeal space with a cystic change and calcification (likely dystrophic) that would likely lead to a main consideration of a benign salivary gland neoplasm. The calcification cannot be used to add specificity to the diagnostic process.

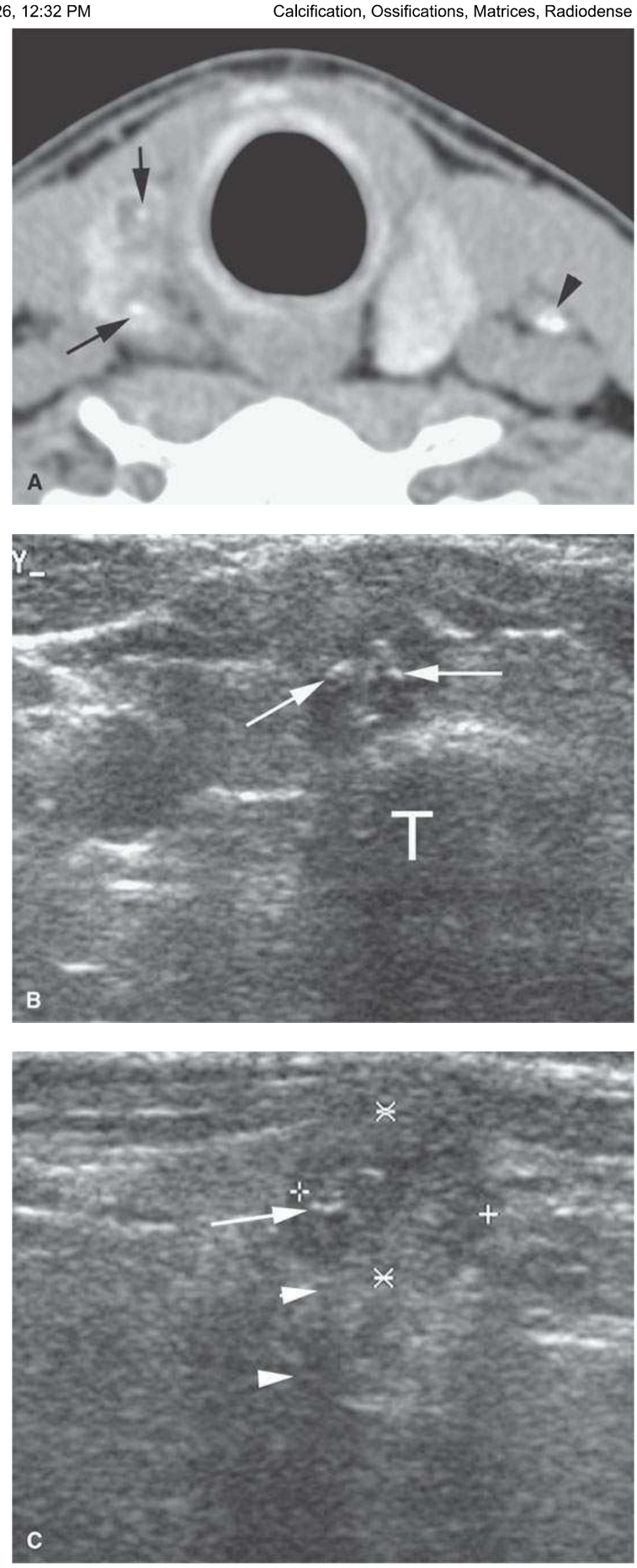

FIGURE 12.30. A: Non–contrast-enhanced computed tomography showing psammomatoid calcifications in the papillary thyroid cancer *(arrows)* and calcified level 6 nodes *(arrowheads)*. High-level echoes in the mass (*arrows* in **B** and **C**) and acoustic shadowing (*arrowheads* in **C**) related to the calcification.

TUMORAL CALCIFICATION

Tumoral calcification may be due to matrix-producing tumors. Most of those tumors are uncommon in the head and neck unless fibrous dysplasia is included in this category. This is discussed more completely in the following section on matrices.

Tumoral calcification is most usually the result of dystrophic calcification in areas of necrosis also known as regressive tumor changes.[10] It can also occur in tumors as part of a reactive change, such as may be the case in thyroid psammoma bodies (Fig. 12.30).[10] Mucoid elements or impacted secretions in tumors can become hardened and mimic calcification or can actually provide a substrate for true calcification; this occurs in salivary and lacrimal gland–origin epithelial neoplasms (Figs. 12.8, 12.25A, 12.31). Such sporadic changes are usually not useful in differential diagnosis and can lead to a mistaken impression that the tumor actually is one that has an identifiable matrix (Fig. 12.29D,E). Examples of reactive or regressive calcification occur in lesions as diverse as retinoblastoma (Fig. 12.29), schwannomas, thyroid and other adenomas/carcinomas (Fig. 12.30), mesenchymal origin sarcomas (Fig. 12.29E), and chordomas.[10]

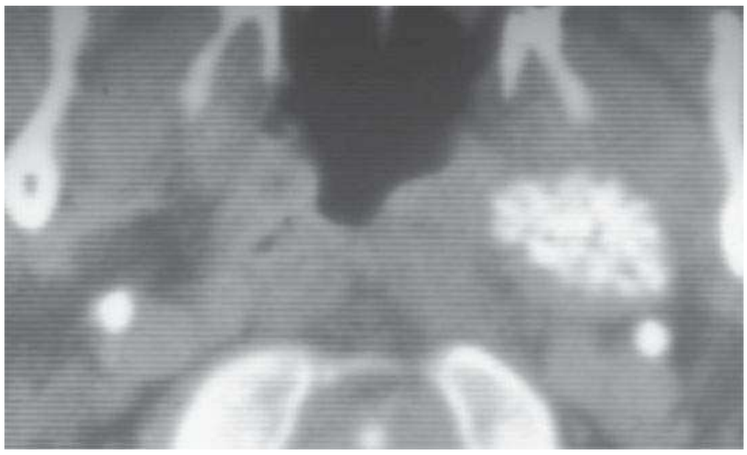

FIGURE 12.31. Calcification in a surgically proven benign mixed tumor of the parapharyngeal space. By its appearance, it more likely is calcification of the chondroid matrix, which can be prominent in these lesions.

CALCIFIED MATRICES

Osteoid, chondroid, and fibrous matrices of a tumor may calcify (Figs. 12.3B,C, 12.14, 12.31, and 12.32). Obvious examples include typical matrix calcification in fibrous dysplasia and the benign and malignant tumors that arise from osteocytes and chondrocytes. Many dental lesions contain cells that will give rise to some type of mineralized matrix. While matrix calcification often leads to a "specific" imaging diagnosis, such specificity imaging observation might not be precisely borne out pathologically (Fig. 12.33). Matrix-producing tumors that appear divergent radiographically may look alike pathologically (Fig. 12.34). Of these, fibrous dysplasia is the most common and most diverse in its appearance (Fig. 12.35) as well as has the ability to mimic more ominous disease processes by its MRI appearance, only to be shown as typically benign and fairly characteristic on CT (Figs. 12.36 and 12.37). Those tumors that may appear to be of one cell line by virtue of the matrix as it appears on imaging may turn out to contain a number of cell lines, with some more aggressive than others pathologically (Fig. 12.14). The best evaluation of matrix-producing tumors usually comes from the comparison of their clinical behavior with their appearance on imaging both correlated with histopathology. Even benign fibro-osseous tumors can show accelerated growth under the hormonal influence of puberty and pregnancy (Fig. 12.38).

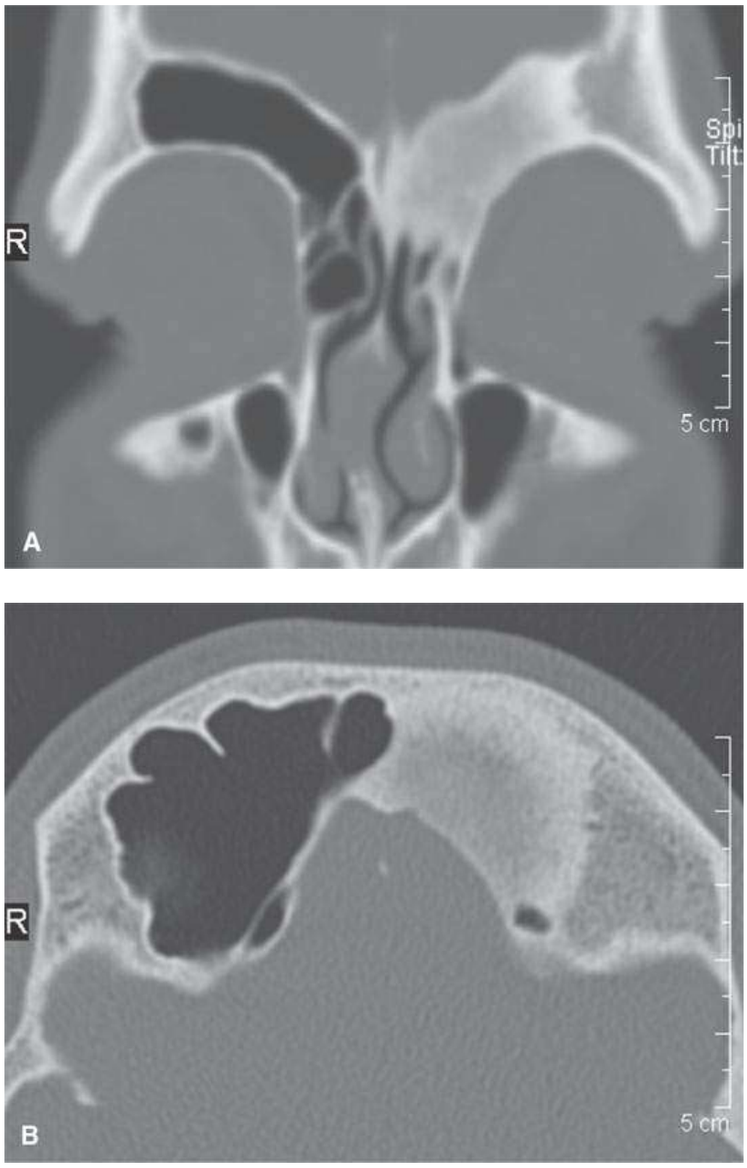

FIGURE 12.32. Mineralized matrices may or may not be specific. **A, B**: essentially diagnostic computed tomography of typical fibrous dysplasia.

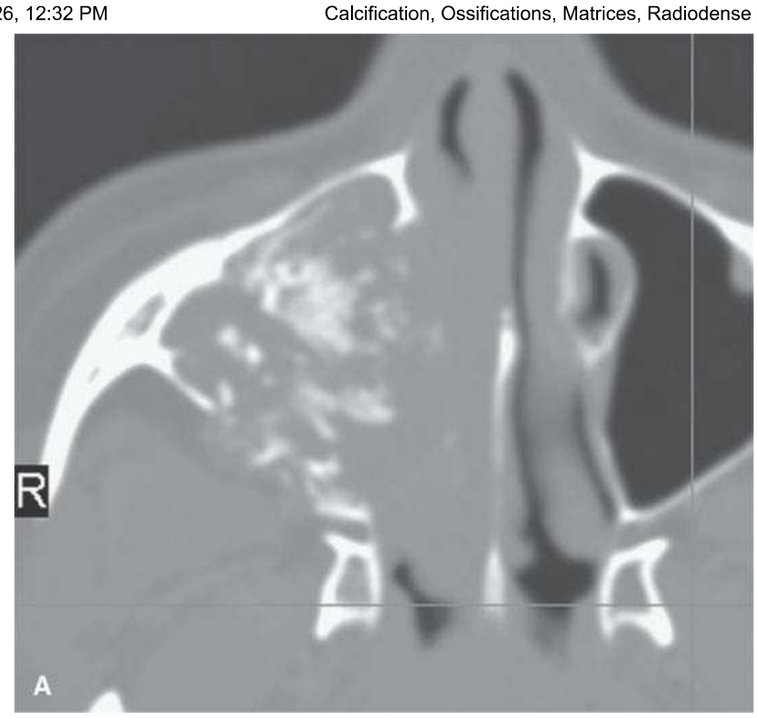
R
A

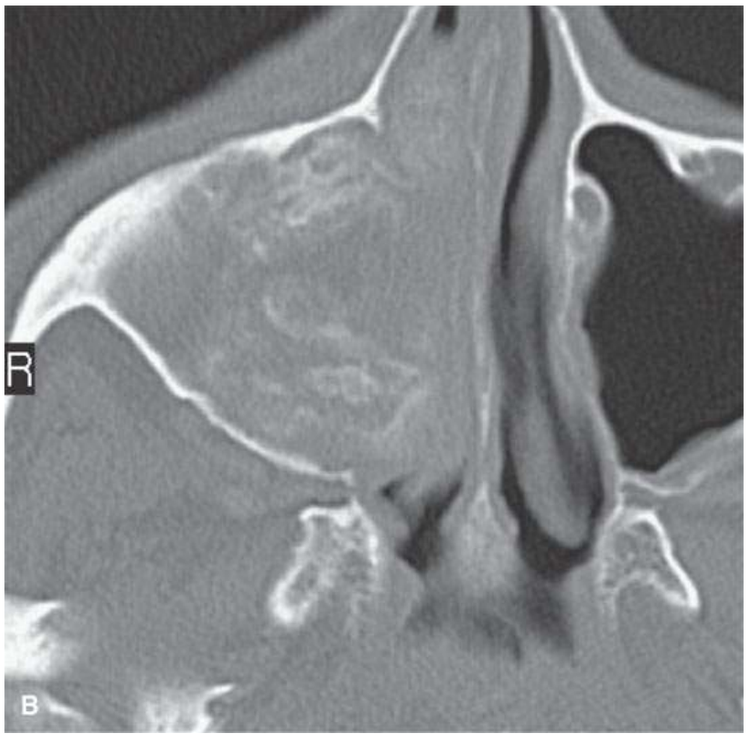
R
B

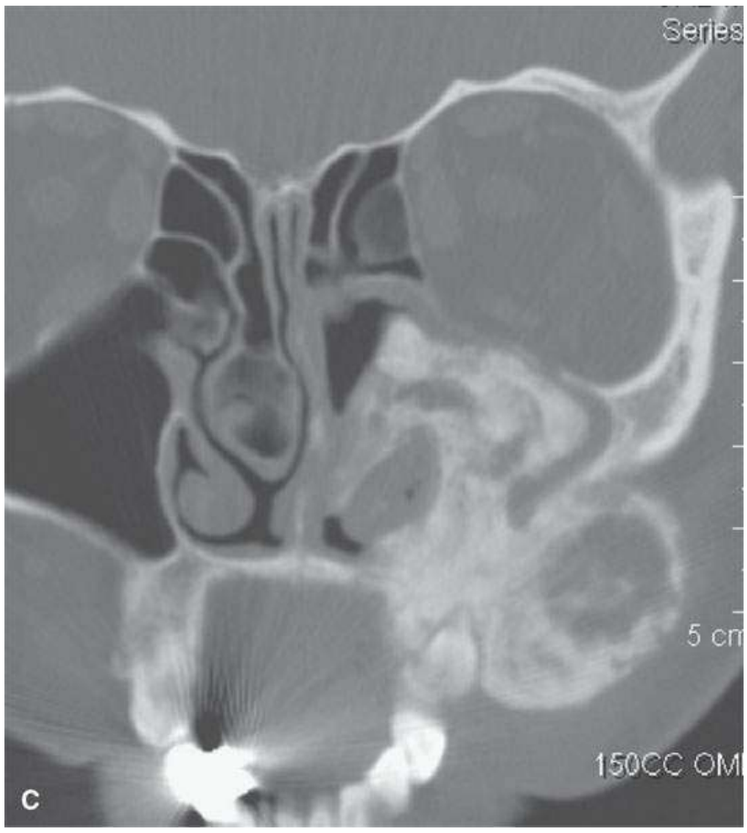

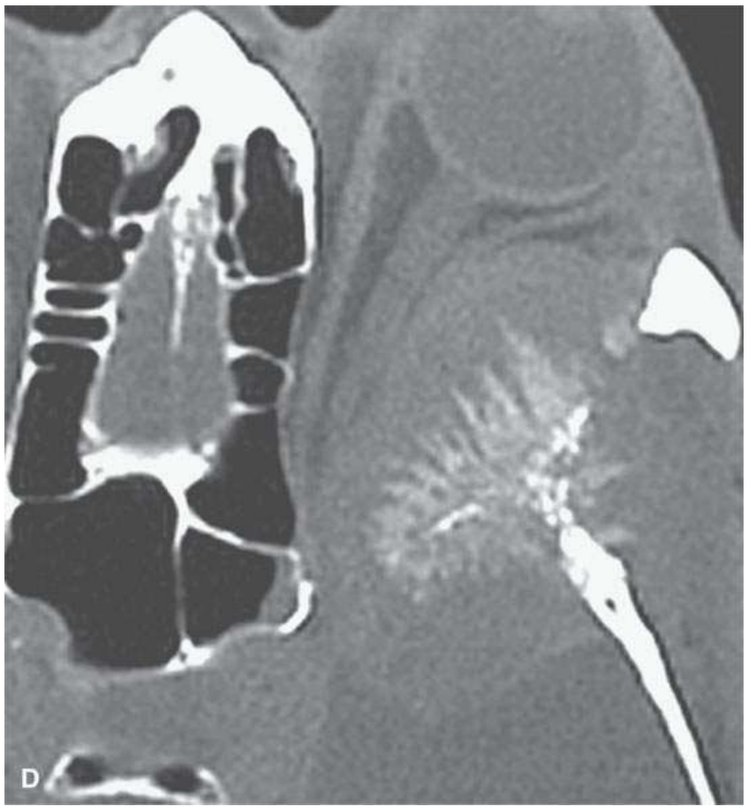

FIGURE 12.33. Mineralized matrices may or may not be specific. **A**: Computed tomography (CT) of a typical osteosarcoma (proven) matrix. **B**: CT of another osteosarcoma (different than in **A**). **C**: CT of what appears to be a osteoid matrix—tumor histologically was mixed Ewing sarcoma and osteosarcoma. **D**: CT finding suggestive of osteosarcoma or highly reactive osteoid matrix in a surgically proven meningioma.

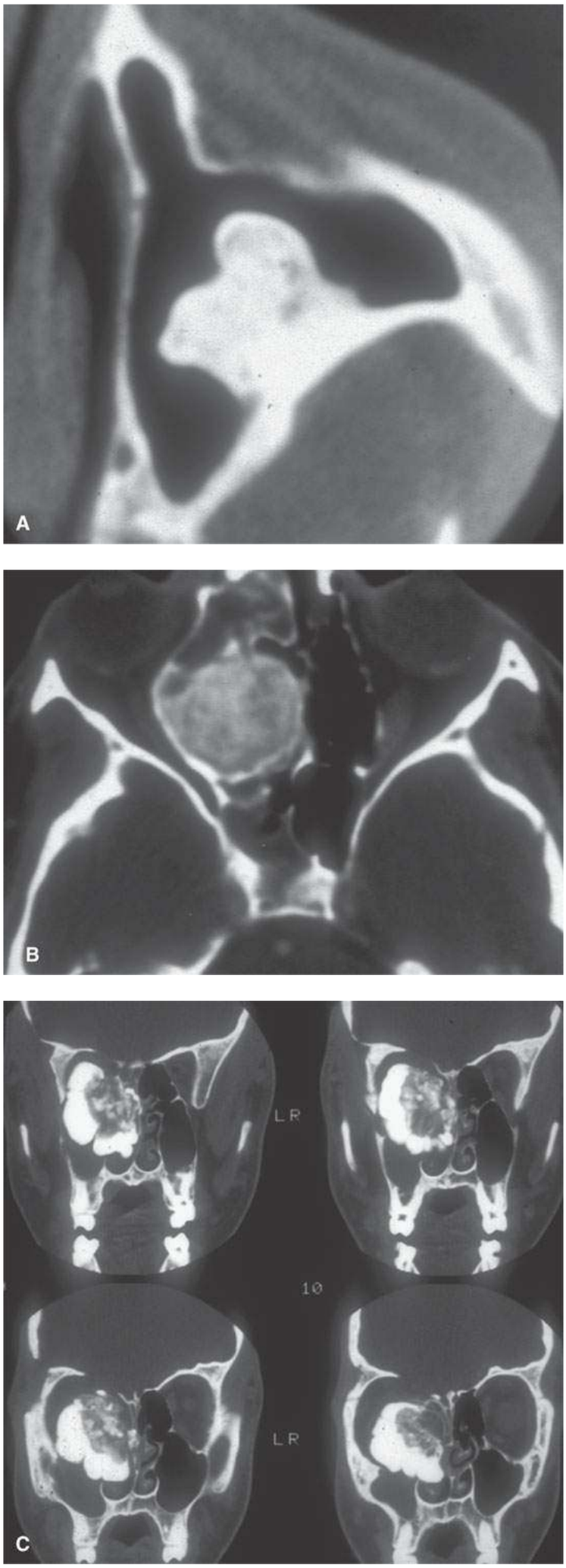

FIGURE 12.34. Various fibroosseous variants—all appear likely pathologically. **A**: Computed tomography (CT) of what was referred to as an osteoma. **B**: CT of what was referred to as an ossifying fibroma. **C**: CT of what was referred to as a fibrous osteoma.

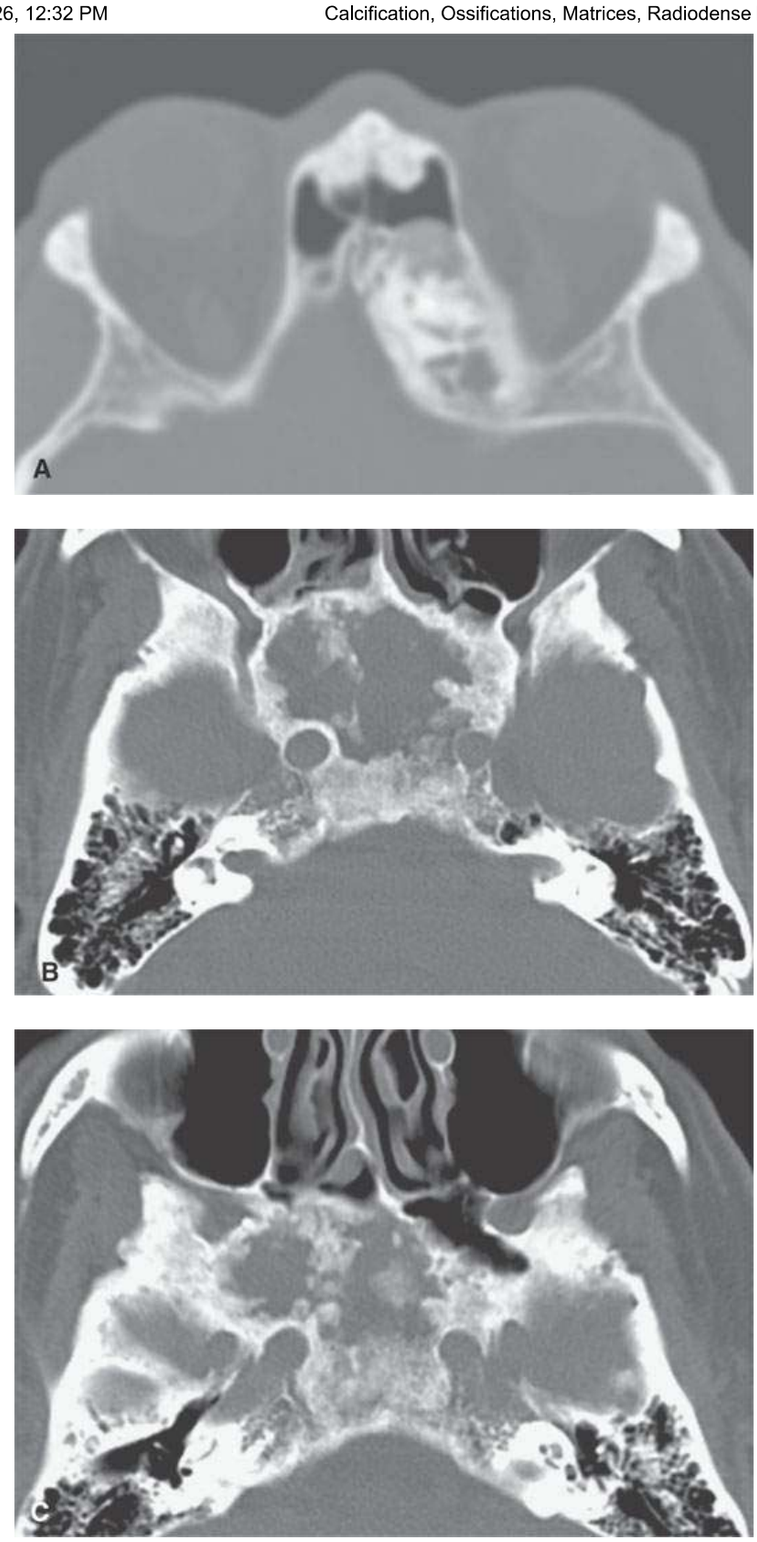

FIGURE 12.35. The fibro-osseous variations of fibrous dysplasia**. A–C:** Computed tomography of fibrous dysplasia in three different patients**.**

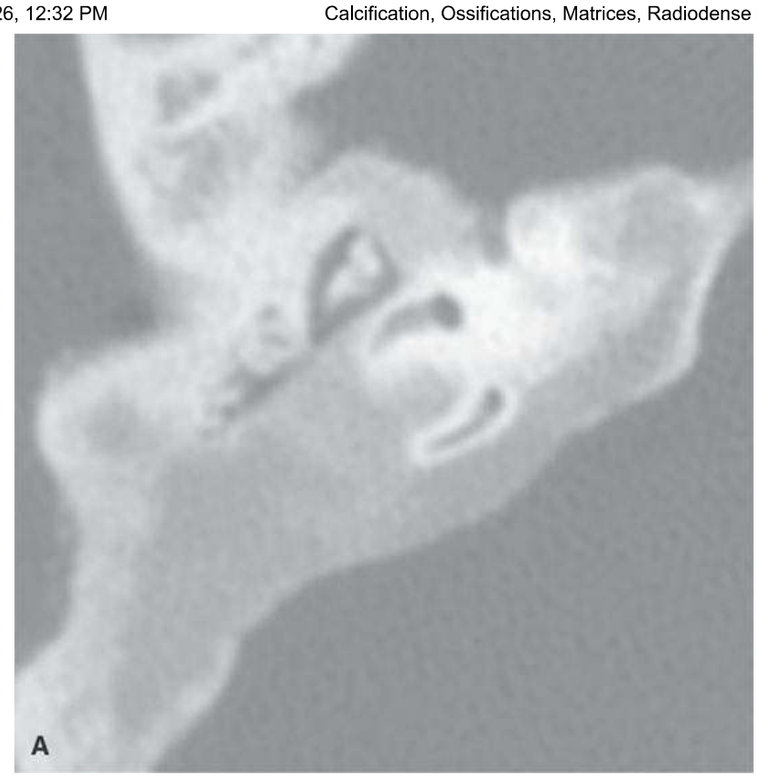
A

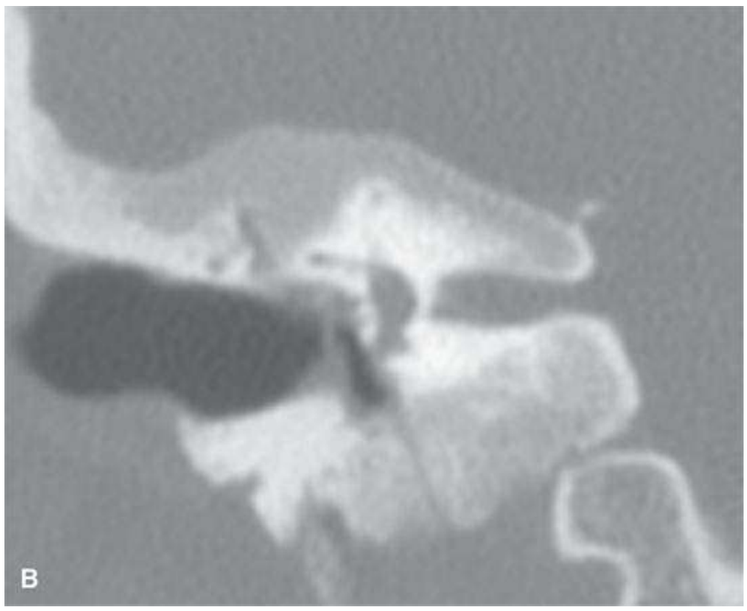
B

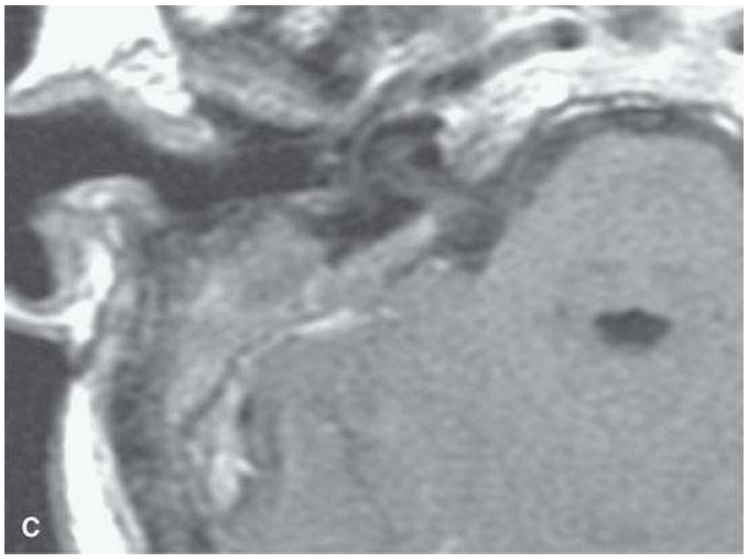
C

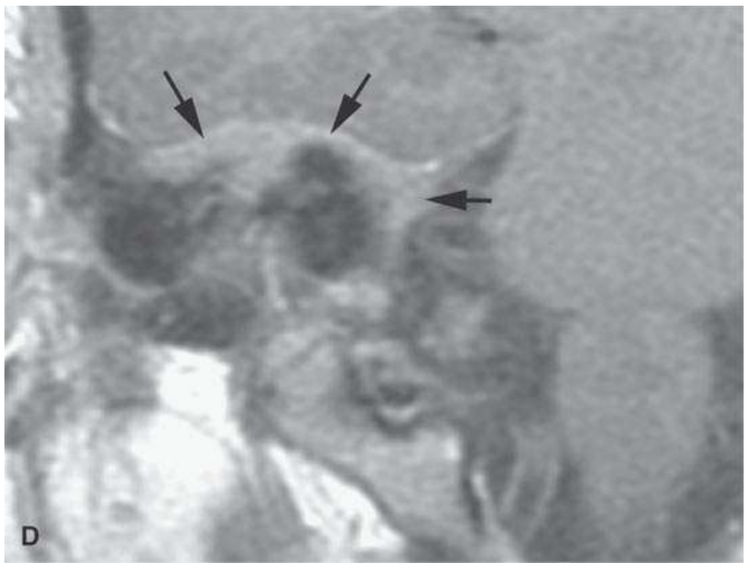

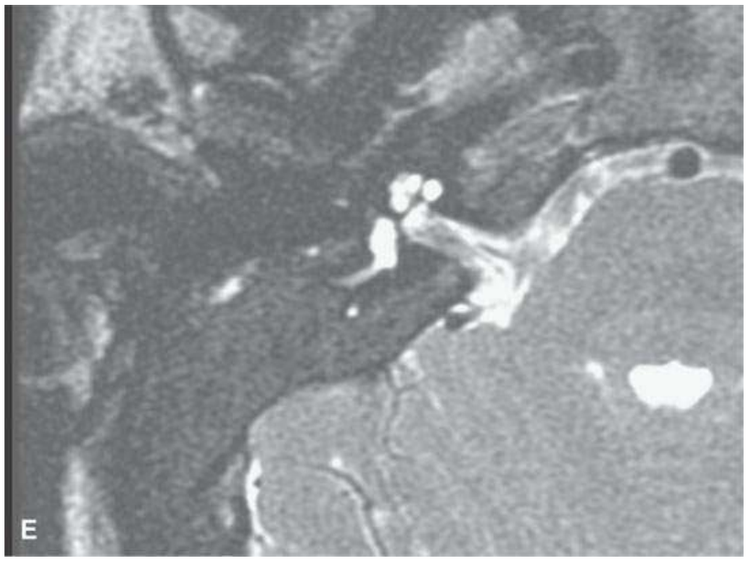

FIGURE 12.36. Fibrous dysplasia of the temporal bone—a simple diagnosis on computed tomography (CT) but more complex and less "recognizable" as such on magnetic resonance imaging (MRI). **A, B:** CT showing typical fibrous dysplasia in a somewhat atypical location—the petrous part of the temporal bone. T1-weighted contrast-enhanced axial **(C)** and coronal **(D)** MRI showing low-grade enhancement that appears to be beyond the expected margin of bone *(arrows)*, but the bone is actually "expanded." The T2-weighted MRI shows low signal of the involved bone, suggesting a fibrous, or at least relatively proton poor or poorly mobile proton, environment in the lesion.

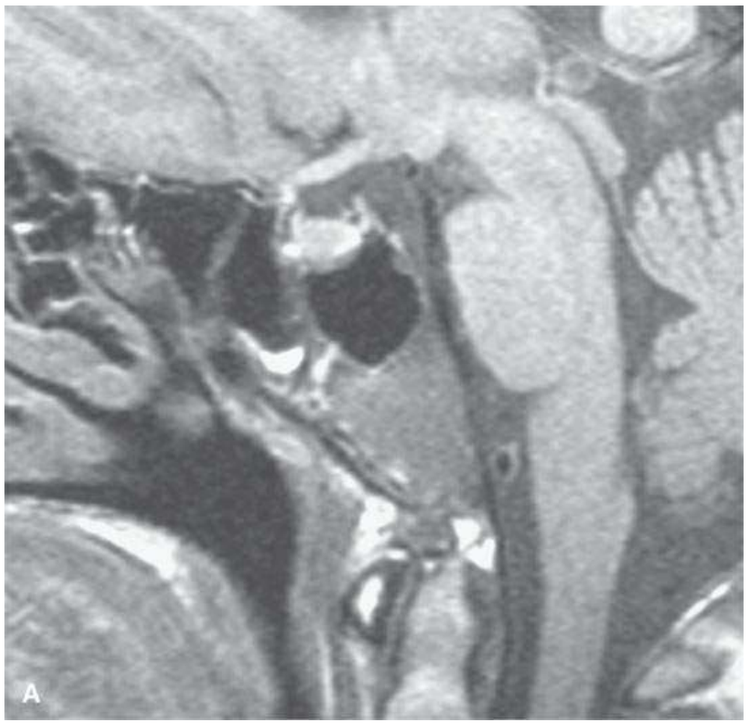

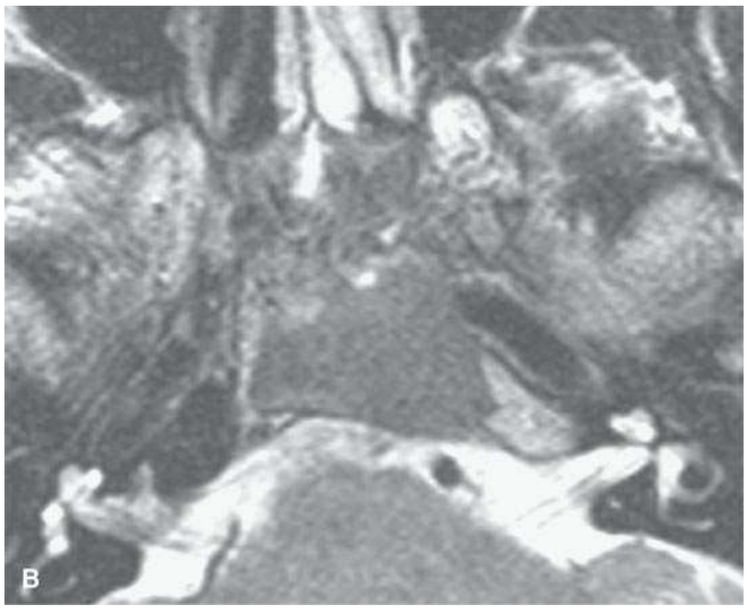

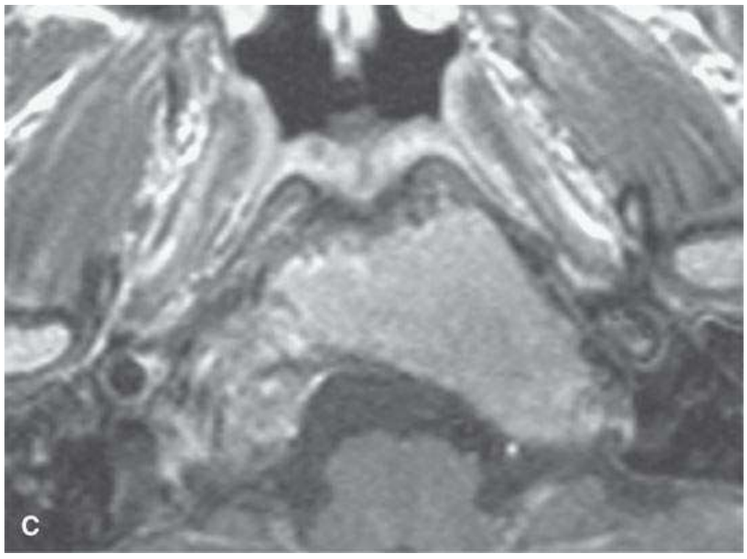

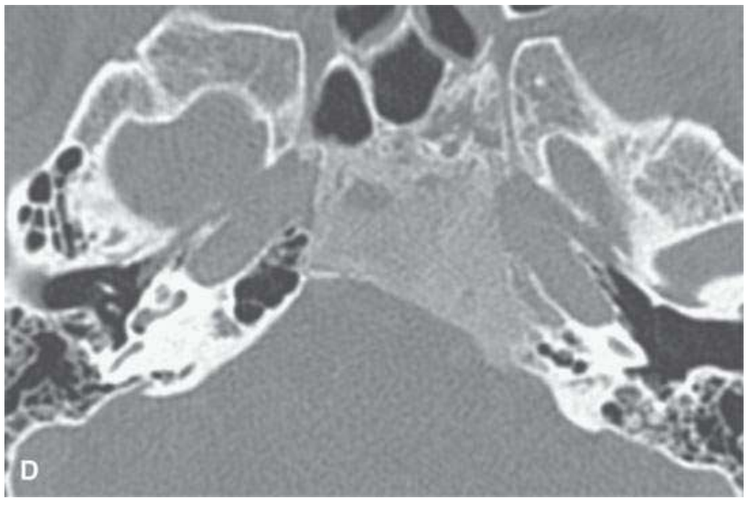

FIGURE 12.37. Fibrous dysplasia of the clivus can mimic more ominous process. **A:** T1-weighted non–contrast-enhanced image shows an "infiltrated"-appearing clivus. **B:** T2-weighted image supports an abnormal marrow space. **C:** T1-weighted contrast-enhanced image shows enhancement (compare with **A**). **D:** Non–contrast-enhanced computed tomography of a typical fibrous dysplasia, although one could think about an osteoblastic metastasis or lymphoma until the expanded appearance of the bone is fully appreciated.

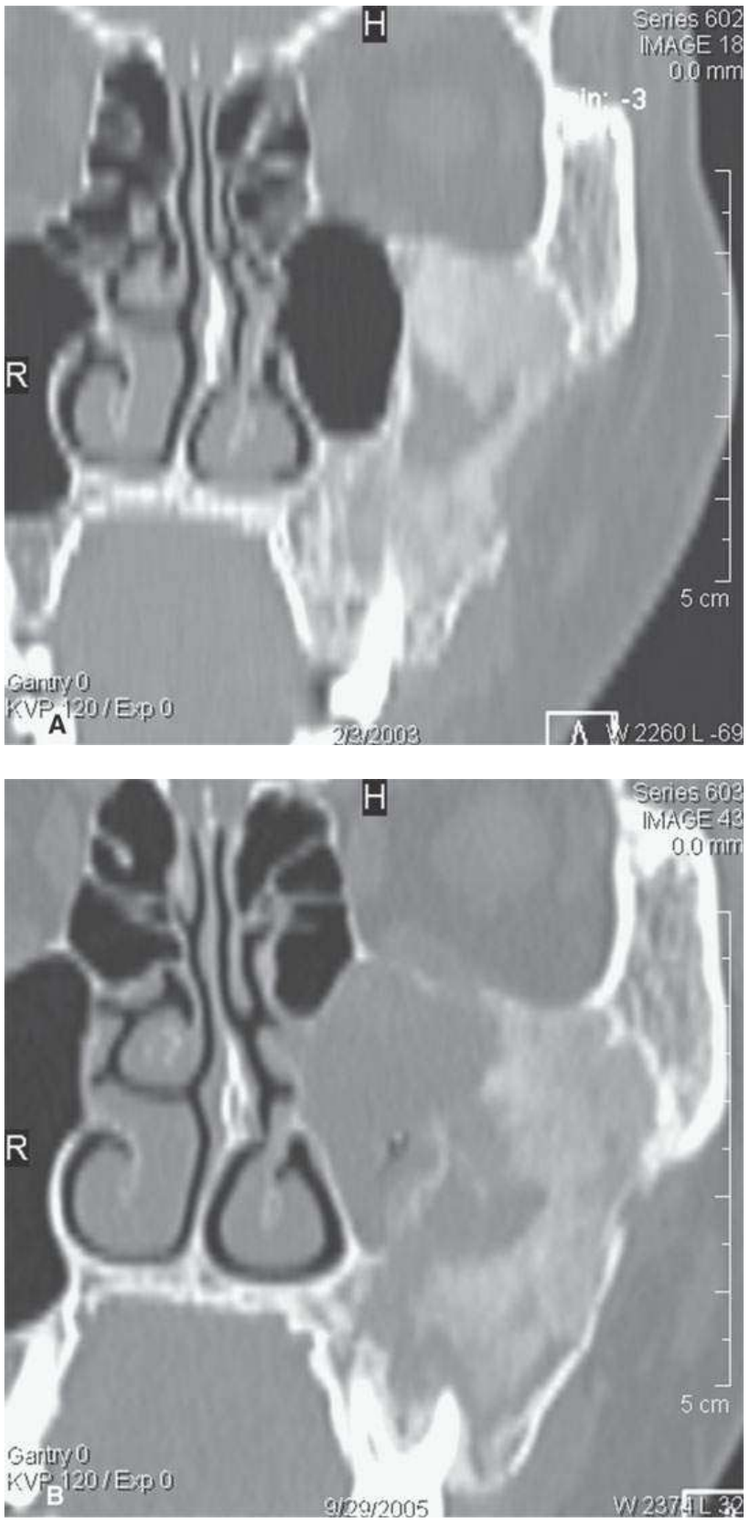

FIGURE 12.38. Fibrous dysplasia of many years duration **(A)** showed rapid growth over about 6 months during pregnancy (B). This stopped after delivery. Relatively rapid progression can also be seen in juvenile aggressive ossifying fibroma without such a "stimulus."

Occasionally, tumors may contain such a matrix prone to calcification. Benign mixed tumor is a good example, with the chondroid component of this tumor producing the explanation for some of the calcification that is occasionally present (Fig. 12.31).10

DISORDERS OF CALCIUM METABOLISM

While these conditions are mainly manifest as abnormalities of both enchondral and membranous bones (Fig. 12.39) in the head and neck region, some will result in abnormal calcium deposition elsewhere.

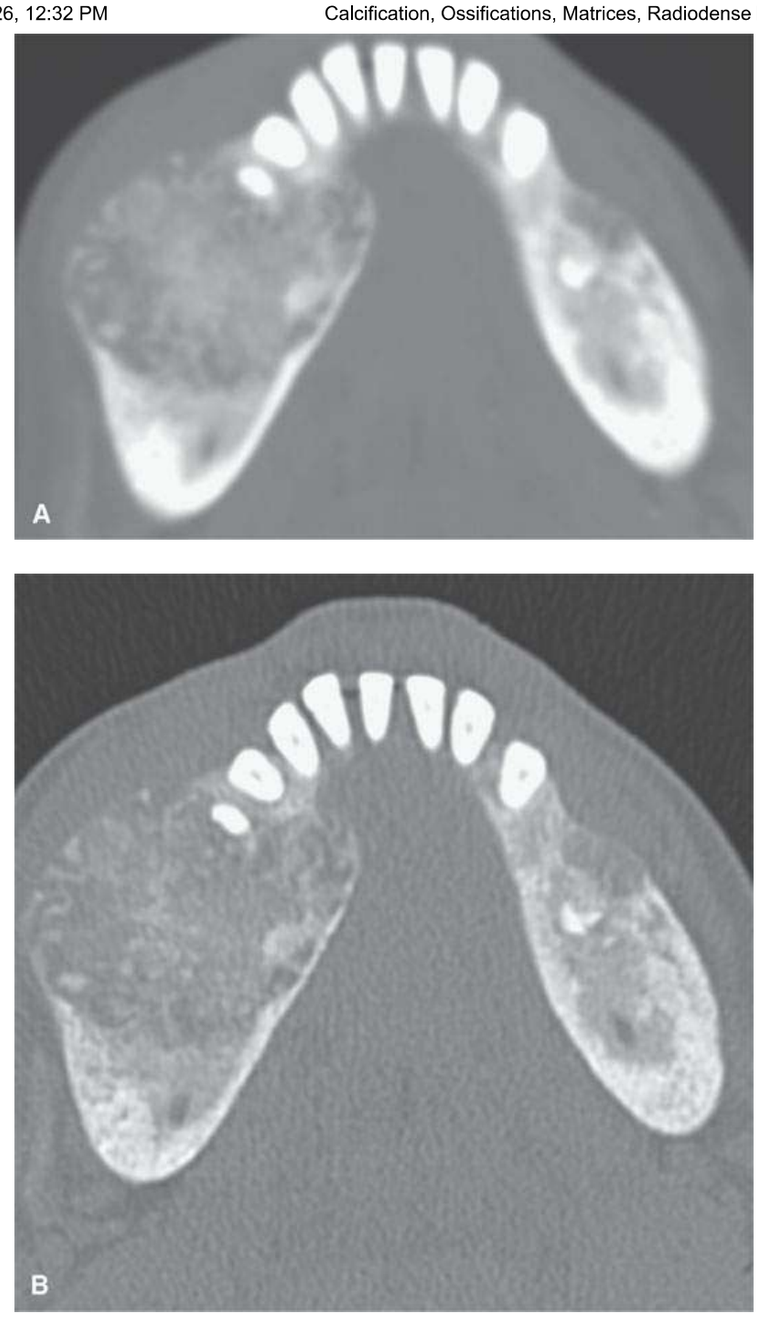

FIGURE 12.39. Computed tomography without **(A)** and with **(B)** bone algorithm reconstruction of a healing brown tumor. Bone algorithms are useful but not essential in the evaluation of mineralized matrices.

Hyperparathyroidism is associated with increased tendency for calcification whether it is at a site of usual physiologic calcification such as the globus pallidus, dystrophic calcification, or a result of abnormal calcium deposition caused by the disease process.

SIALOLITHIASIS AND OTHER "STONES"

The detection of stones in acute and subacute sialoadenitis is a critical observation for proper diagnosis. MR is simply not reliable, and this feature alone makes CT the proper choice when evaluating major salivary gland masses or problems that have any hint of an inflammatory or infectious etiology based on the clinical presentation (Fig. 12.3A).

Phleboliths may be detectable as signal void siting in the blood pool of a vascular malformation, but they are much easier appreciated as such on CT (Fig. 12.40). This is rarely an important issue since the diagnosis of a slow-flow vascular malformation is almost always known or anticipated prior to imaging.

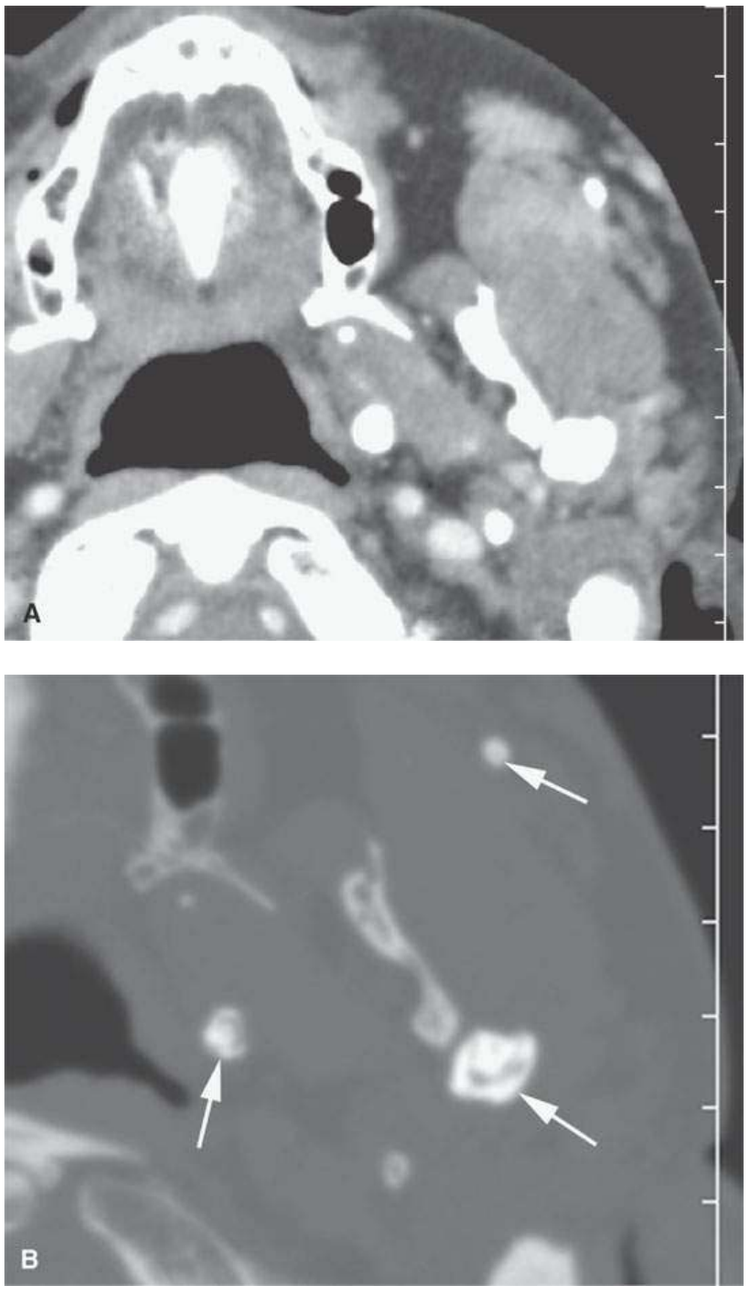

FIGURE 12.40. Contrast-enhanced computed tomography of the phleboliths securing the diagnosis of a venolymphatic malformation—a strength of computed tomography in a lesion usually better evaluated with magnetic resonance imaging.

OTHER CONDITIONS WHERE THE PATTERN OF CALCIFICATION DIRECTS THE DIAGNOSTIC PROCESS

There are other situations where the proper recognition of calcification enlightens the diagnostic process. These include but are not limited to the following:

- Drusen that can mimic papilledema clinically and are unmistakable as seen on CT (Fig. 12.41).11

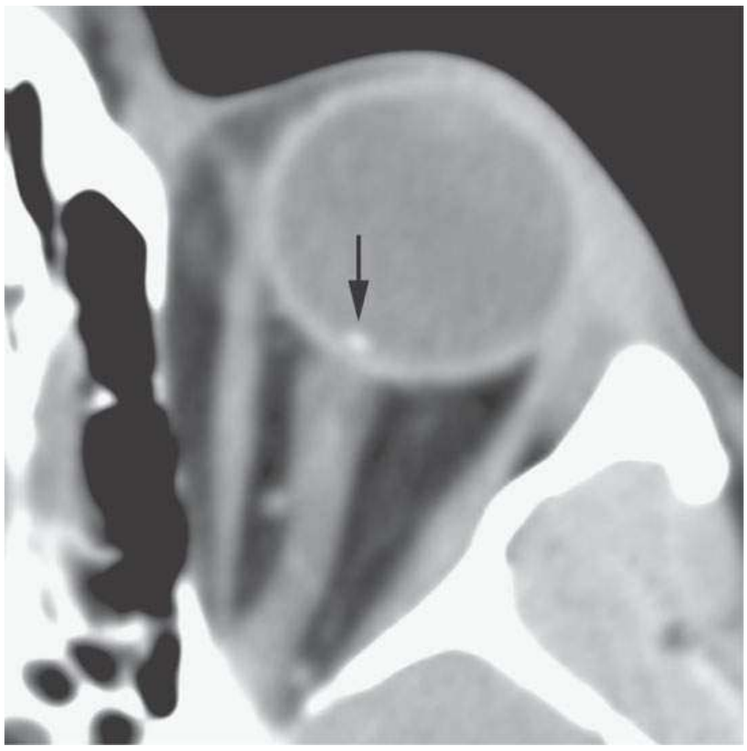

FIGURE 12.41. Computed tomography of an optic nerve Drusen *(arrow)*.

- Calcification that may be seen in association with vasculopathy, such as Sturge-Weber and the related choroidal vascular malformations or just the isolated choroidal osteoma that may appear more “ominous” on MRI (Fig. 12.42).12

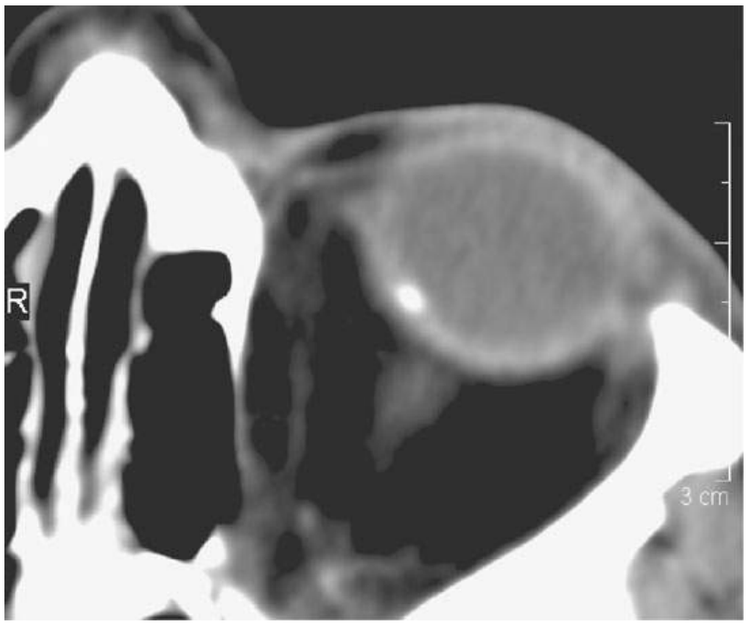

FIGURE 12.42. Computed tomography of a choroidal osteoma.

- Calcifications that may be seen in association with metabolic bone disease, crystalline arthropathy, or bone and joint disease such as osteochondromatosis and markedly narrow the differential considerations (Fig. 12.43). Such information may also help the evaluation of more routine disease such as degenerative changes (Fig. 12.1).

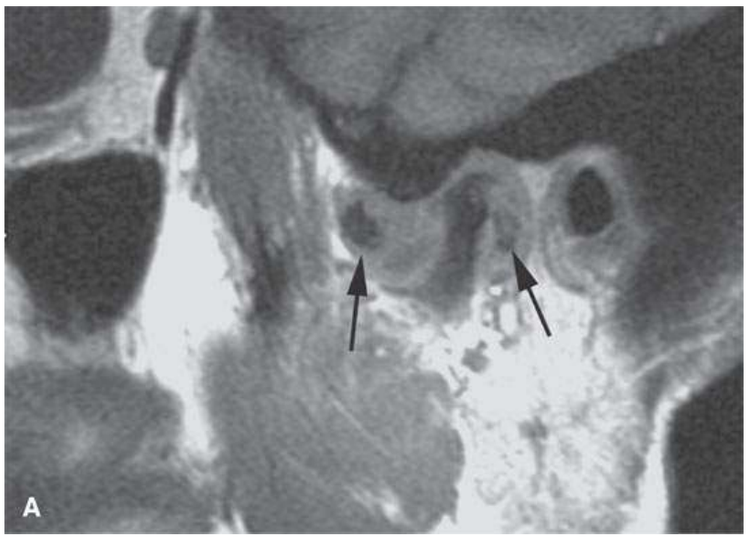

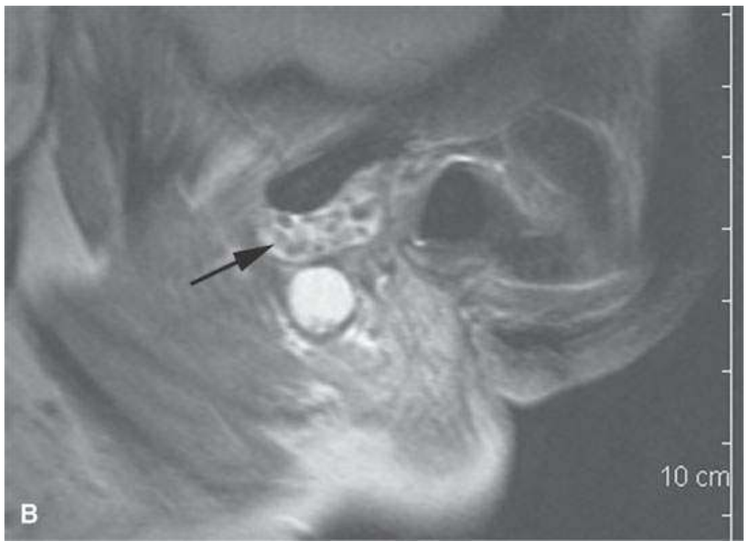

FIGURE 12.43. Magnetic resonance imaging of temporomandibular joint osteochondromatosis. The T1-weighted image in **(A)** shows signal voids in the joint *(arrows)* and a likely distended joint capsule. The T2-weighted image in (b) shows the distended joint capsule *(arrow)* and multiple areas of ossific density as voids with the pathologic joint space.

Suggested Readings

Heffner DK. Allergic fungal sinusitis is a histopathologic diagnosis; paranasal mucocele is not. *Ann Diagn Pathol*. 2004;8(5):316–323.

References

1. Wakisaka N, Miwa T, Yoshizaki T, et al. Cricoid ossification mimicking an impacted foreign body. *J Laryngol Otol*. 2006;120(7):E24.

2. Terada H, Barkovich AJ, Edwards MS, et al. Evolution of high-intensity basal ganglia lesions on T1-weighted MR in neurofibromatosis type 1. *AJNR Am J Neuroradiol*. 1996;17(4):755–760.

3. Daghighi MH, Rezaei V, Zarrintan S, et al. Intracranial physiological calcifications in adults on computed tomography in Tabriz, Iran. *Folia Morphol (Warsz)*. 2007;66(2):115–119.

4. Arasaratnam S, Abdullah BJ, Fernandez V. Calcified vertical plate of the cricoid—A rare pitfall in the diagnosis of an oesophageal foreign body. *Med J Malaysia*. 1998;53(3):290–292.

5. Ojiri H, Mendenhall WM, Stringer SP, et al. Post-RT CT results as a predictive model for the necessity of planned post-RT neck dissection in patients with cervical metastatic disease from squamous cell carcinoma. *Int J Radiat Oncol Biol Phys*. 2002;52(2):420–428.

6. Stary HC. Natural history of calcium deposits in atherosclerosis progression and regression. *Z Kardiol*. 2000;89(suppl 2):28–35.

7. DelGaudio JM, Swain RE Jr, Kingdom TT, et al. Computed tomographic findings in patients with invasive fungal sinusitis. *Arch Otolaryngol Head Neck Surg*. 2003;129(2):236–240.

8. Yoon DY, Lee JW, Chang SK, et al. Peripheral calcification in thyroid nodules: Ultrasonographic features and prediction of malignancy. *J Ultrasound* Med. 2007;26(10):1349–1355.

9. Wang N, Xu Y, Ge C, et al. Association of sonographically detected calcification with thyroid carcinoma. *Head Neck*. 2006;28(12):1077–1083.

10. Mizerny BR, Kost KM. Chordoma of the cranial base: The McGill experience. *J Otolaryngol*. 1995;24(1):14–19.

11. Baehring JM, Biestek JS. Optic nerve head Drusen mimicking papilledema. *J Neurooncol*. 2005;72(1):47.

12. Bodensteiner JB, Roach ES, eds. Sturge-Weber syndrome: Introduction and overview. In: *Sturge-Weber syndrome*. Mount Freedom, NJ: Sturge-Weber Foundation; 1999:1–10.

Related Posts:

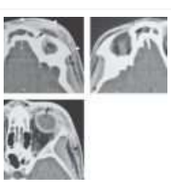
Preseptal Compartment:

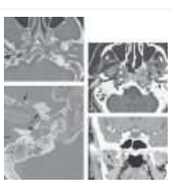
Necrotizing ("Malignant") Otitis

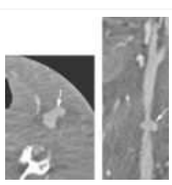
Cervicothoracic Junction: Brachial

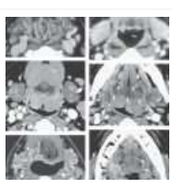
Oropharynx: Introduction

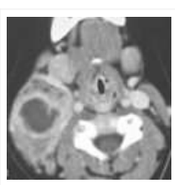
Branchial Apparatus

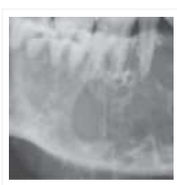
Mandible and Maxilla:

May 14, 2017 | Posted by admin in HEAD & NECK IMAGING | Comments Off